

# A Perfectly Distributable Quantum-Classical Algorithm for Estimating Triangular Balance in a Signed Edge Stream

STEVEN KORDONOWY, Fujitsu Research of America Inc., Santa Clara, USA and University of California at Santa Cruz, USA

BIBHAS ADHIKARI and HANNES LEIPOLD, Fujitsu Research of America Inc., Santa Clara, USA

We develop a perfectly distributable quantum-classical streaming algorithm that processes signed edges to efficiently estimate the counts of triangles of diverse signed configurations in the single pass edge stream. Our approach introduces a quantum sketch register for processing the signed edge stream, together with measurement operators for query-pair calls in the quantum estimator, while a complementary classical estimator accounts for triangles not captured by the quantum procedure. This hybrid design yields a polynomial space advantage over purely classical approaches, extending known results from unsigned edge stream data to the signed setting. We quantify the lack of balance on random signed graph instances, showcasing how the classical and hybrid algorithms estimate balance in practice.

**Keywords:** Quantum-Classical Algorithms, Quantum Streaming, Signed Networks, Structural Balance, Perfectly Distributable Quantum Algorithms

## 1 Introduction

Computing statistical quantities for summarizing large-scale data, particularly large networks, under memory-constrained resources has become increasingly important in the era of big data. Quantum computing systems could mature to play a pivotal role in this evolving landscape [1]. For example, in the single pass streaming setting, quantum devices have shown to provide space advantages in a host of settings, including one-way Boolean functions [2], triangle counting [3], and directed maxcut [4]. Despite the abundance of distributed computing frameworks for classical streaming algorithms, the literature lacks quantum distributed frameworks for quantum streaming algorithms. In this paper, we attempt to fill this gap by developing a quantum-classical streaming algorithm for counting triangles in a signed edge stream implemented in a distributed computing setup.

Triangle finding and counting in the edge streaming graph model is a fundamental problem due to its importance in network analysis and algorithms. In this model, edges of a graph arrive sequentially as a stream, and algorithms are required to detect or estimate the number of triangles using sublinear space, often in a single pass. Early work established both lower bounds and randomized algorithms for triangle counting in insertion-only streams, highlighting the inherent space accuracy trade-offs [5]. Subsequent approaches introduced sampling-based and sketching techniques to approximate triangle counts in massive graphs [6, 7]. The algorithm described in Ref. [8], henceforth the Jayaram-Kallaughner (JK) algorithm, is provably optimal in space (up to polylogarithmic factors), settling the problem on classical triangle counting in the edge stream setup by matching known lower bounds under standard parameterizations of the problem. In Ref. [3], Kallaughner introduced a quantum-classical algorithm for approximating triangle counts that results in a polynomial space advantage over the classically-optimal JK algorithm.

In this paper, we consider the single-pass insertion-only signed graph stream model in which each signed edge appears only once. Signed graphs have two types of edges: positive and negative edges (see Section 2 for further details). Applications of signed graphs and balance measures are widespread. In social network analysis, they model trust/distrust relations and help identify polarized communities [9, 10]. In international relations, signed networks capture alliances and conflicts among countries, with balance dynamics linked to stability [11, 12]. In finance,

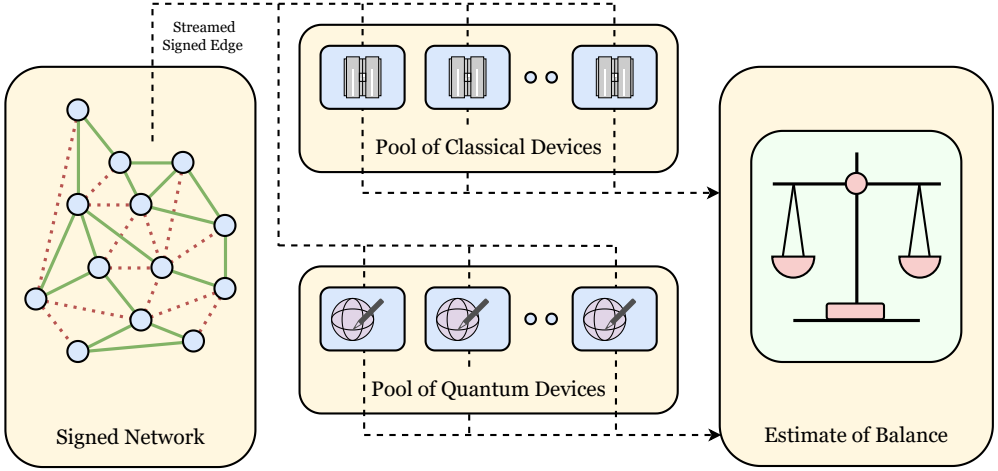


Fig. 1. **Quantum-Classical Estimation of Balance in the Streaming Model.** An overview of our hybrid quantum-classical algorithm for estimating balance.

signed correlation graphs describe co-movements and anti-movements of asset returns, with balance analysis providing insights into systemic risk and market stability [13–18]. In biology, signed networks model cooperative and competitive interactions in gene regulatory and protein networks [19, 20]. In physics and complex systems, balance theory underpins models of consensus and cooperation under antagonistic interactions [21, 22].

In the classical setting, we extend the classically-optimal streaming JK algorithm for triangle counting in edge streams to the setting of signed edge streams and we call it *signed JK algorithm*. In this model, each edge in the stream is associated with a sign, and consequently, triangles can be classified into four distinct types (see Figure 2). This introduces additional challenges, as the algorithm must track the product of edge signs in order to correctly identify the type of each triangle during query processing. The resulting estimates of the different triangle types are then used to approximate the degree of balance of the underlying signed graph, as defined by the triangular measure of balance.

Further, we extend the area of space advantage from quantum sketchpads for important and realistic data streaming setting by developing an algorithm for counting triangles for *signed networks*, focusing specifically on the statistical characterization of *balance*. We then present a hybrid quantum-classical algorithm that gives a quantum polynomial advantage over the signed JK algorithm. The proposed algorithm relies on two complementary estimators: a quantum estimator and a classical estimator. The quantum estimator employs a collection of quantum processors, each performing analogous tasks involving sampling and the execution of quantum queries, while the classical estimator consists of a collection of classical processing units carrying out a similar sampling-based procedure. These two estimators play complementary roles within the hybrid framework. In particular, triangles of a given type that may be missed by the quantum estimator due to the probabilistic nature of quantum measurements are detected by the classical estimator with nonzero probability. The overall hybrid approach is inspired by the classical–quantum algorithm for estimating triangle counts in unsigned edge streams proposed in Ref. [3]. The primary technical challenge addressed in this work lies in the construction of a quantum sketch register capable of encoding signed edges observed in the signed edge stream, together with the design of appropriate

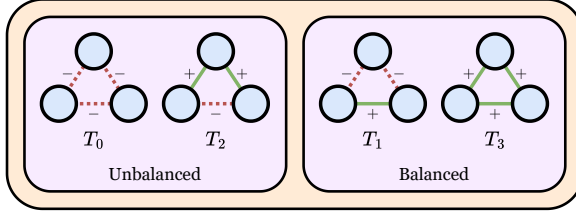


Fig. 2. **Triangle Types and their Balance in a Signed Network.** Triangle types labeled by their number of positive edges, with triangles with odd number of plus edges categorized as balanced while those with even positive edges are categorized as unbalanced. Under structural balance theory, real-life network dynamics may evolve towards more balanced local substructures. As such, counting triangle types is essential for analyzing networks.

POVM operators for performing quantum queries on this register. A circuit-level description of the proposed procedure is provided in Figure 3. We then use this approximation of triangle types to estimate the balance of networks.

Finally, we introduce a distributed computing framework that integrates classical and quantum processors to implement the proposed hybrid quantum-classical algorithm for estimating different types of signed triangles which is leveraged to approximate the structural balance of the underlying signed graph. To evaluate performance, we generate signed edge streams from random signed graphs and compare the proposed hybrid approach with its purely classical counterpart using state-vector simulations. To the best of our knowledge, this work represents the first instance in the literature of a distributed quantum-classical computing model designed specifically for implementing streaming algorithms on graph streams. The framework developed in the paper is presented in Figure 1.

We emphasize that the proposed distributed framework is fundamentally different from standard distributed frameworks. Classical approaches rely on interconnected machines and must address challenges such as *parallelism*, *load balancing*, and *network efficiency* [23]. Standard distributed quantum computing typically focuses on quantum networking challenges, including implementing quantum operations such as quantum gates across multiple quantum processing units (QPUs). A *perfectly distributable* quantum algorithm is one in which each processor contributes independently without inter-processor communication [24]. We establish that both the hybrid algorithm of Ref. [3] and the algorithm proposed here fall into this category: a pool of QPUs and classical processing units (CPUs) operates independently, and the final estimate is obtained via combined classical post-processing of outcomes (see Section 5).

## 2 Graph streams, triangles and balance of Signed Graphs in a Stream

In this section, we briefly review of existing distributed computing frameworks for graph streams and structural balance theory of signed graphs. We also include a discussion on the set of parameters used in sequel.

### 2.1 Graph Streams

In classical streaming data analysis model, the *graph streaming model* extends the classical data stream paradigm to graph-structured data, where vertices and edges arrive sequentially as a stream. In this setting, the input graph is too large to store explicitly in memory, and algorithms are required to process updates, such as edge insertions, deletions, or weight changes, using sublinear space

and typically a single or a small number of passes over the stream. Depending on the update rules, graph streams are commonly classified into insertion-only, turnstile, and dynamic models. The graph streaming framework has become a central tool for analyzing massive networks arising in social media, communication systems, and biological data, establishing space-accuracy tradeoffs for fundamental graph problems [25–29].

Classical streaming algorithms, in particular, graph streaming algorithms are deployed naturally in a distributed computing framework for massive graph analytics, with theoretical guarantees on space, communication complexity, and approximation accuracy [23, 25, 26, 30]. Several open-source distributed graph processing frameworks such as the vertex-centric programming models: Google’s Pregel [31], Pregel+ [32], GraphLab [33], PowerGraph [34], Giraph [35], and GPS [36] have been developed considering the abstraction of parallel looping, message receiving and sending, and broadcasting. Besides, edge-centric and subgraph-centric distributed graph processing frameworks are proposed to boost performance that require edge lists and bypassing random memory accesses associated with vertices, such as X-Stream [37], WolfGraph [38], Giraph++ [39], GoFFish [40], Blogel [41].

## 2.2 Signed Graphs and Signed Triangles

A signed graph  $G = (V, E, \sigma)$  is a graph where each edge  $(i, j) \in E$  is assigned a sign  $\sigma(i, j) \in \{+1, -1\}$ , representing positive (friendly, cooperative, positively correlated) or negative (hostile, antagonistic, negatively correlated) relationships [42, 43]. A signed network can be analyzed by counting the number of small substructures contained in it; the simplest example being the number of triangles. Since the network is signed, the type of triangles are characterized by the sign of the three edges in the triangle, as depicted in Figure 2. There are four types of triangles in a signed graph, depending on the number of *positive* edges in the triangle. Define the enumeration of each type of triangle as

$$T_j, \text{ the number of triangles with } j \text{ positive edges in } G. \quad (1)$$

Then the total number of triangles is the sum of each type:

$$T = T_0 + T_1 + T_2 + T_3, \text{ the number of triangles in } G. \quad (2)$$

## 2.3 Structural Balance Theory

The classical notion of balance, introduced by Harary, states that a signed graph is balanced if its vertex set can be partitioned into two disjoint subsets such that all positive edges lie within the subsets and all negative edges lie between them. Equivalently, a signed graph is balanced if every cycle has a positive sign, i.e., the product of the edge signs along the cycle is +1.

Several quantitative measures of balance have been proposed. One widely used measure is the *balance index*, defined as

$$\mathcal{B}(G) = \frac{\#\{\text{balanced cycles in } G\}}{\#\{\text{total cycles in } G\}}, \quad (3)$$

which captures the proportion of balanced structures in the network [44]. Another is the *frustration index*, which is the minimum number of edge sign changes (or deletions) required to make the graph balanced [45].

Then, in structural balance theory, triangles of types  $T_1$  and  $T_3$  are balance, whereas triangles of type  $T_0$  and  $T_2$  are unbalance. Thus, a balance signed graph has triangles of types  $T_0$  and  $T_2$  only, and hence lack of balance of a signed graph can be estimated by counting all types of triangles in

the graph. In particular, the *triangular index of balance* of a signed graph  $G$  defined as

$$\mathcal{B}_\Delta(G) = \frac{\#\{\text{balanced triangles in } G\}}{\#\{\text{total triangles in } G\}}. \quad (4)$$

Since a triangle is a cycle with three nodes,  $\mathcal{B}_\Delta$  is a special type of  $\mathcal{B}$  (see Eq. (3)).

## 2.4 Parameter Approximation in the Stream

A memory limited device does not have access to the entire input data when solving a problem, since the data might be too large to fit into memory at once, such as in very large social media networks, or due to the nature of the data is that it comes in periodically throughout a period of time, such as in trades in a financial system. In the single-pass streaming setting, we are given a stream  $S = ((uv, \sigma_{uv})_i)_{i=1}^m$  composed of edges  $uv \in E(G)$  and their sign  $\sigma_{uv} \in \{+1, -1\}$ . We wish to (approximately) count  $T_j$  (from Eq. (1)) in the network  $G$ . We work in the insertion-only model in which edges are processed one at a time and are never deleted. Given error parameters  $\epsilon, \delta \in (0, 1]$ , the task is to find a  $(1 \pm \epsilon)$ -multiplicative approximation of  $T$  with probability  $1 - \delta$  using as few space resources as possible.

Any algorithmic approximation guarantee should be independent of the ordering of  $S$ . Indeed, to show worst-case guarantees, one may construct adversarial orderings of  $S$ . In order to construct hard graph instances, we define these standard graph parameters for a graph  $G$ :

$$\begin{array}{ll} n := |V|, \text{ number of nodes in the graph} & m := |E|, \text{ number of edges in the graph} \\ \Delta_V, \text{ maximum number of triangles} & \Delta_E, \text{ maximum number of triangles} \\ \text{incident on any node} & \text{incident on any edge} \end{array}$$

The space complexity for state-of-the-art streaming algorithms for triangle counting are given with respect to these parameters. Note that  $T, \Delta_E, \Delta_V$  are not known ahead of time, since that would defeat the purpose of the algorithm.

Ref. [1] provides a framework for a hybrid quantum-classical algorithm to approximate problems that can lead to better algorithms than purely classical solutions.

## 3 A Purely-Classical Streaming Algorithm for Signed Triangle Counting

Inspired by the optimal classical streaming JK algorithm proposed for (unsigned) edge stream in Ref. [8], we develop a streaming algorithm for estimating number of triangles of type  $T_1$  in a signed edge stream. This algorithm can be trivially adapted to count any (or all)  $T_j$  types.

We first briefly recall the streaming JK algorithm. Prior to their work, several upper and lower bounds for triangle counting in insertion-only streams and for linear sketching algorithms had already been established; see Ref. [8] and the references therein. The key insight underlying their approach is the following: given three edges  $uv, vw, wu \in E$  arriving sequentially in a stream, if the first two edges  $uv$  and  $vw$  are sampled and stored, then upon observing the completing edge  $wu$ , the presence of the triangle  $uvw$  in the underlying graph  $G$  can be detected.

However, naive random edge sampling alone generally leads to suboptimal performance. To overcome this limitation, Jayaram and Kallaugher introduce a carefully parameterized sampling strategy that combines both edge and vertex sampling. Specifically, edges are sampled with probability  $p_E$ , while vertices are sampled independently with probability  $p_V$ , and triangles are counted when they close sampled wedges. The sampling probabilities are chosen as

$$p_E = \frac{\Delta_V}{T}, \quad p_V \geq \max \left\{ \frac{\Delta_V}{\Delta_E}, \frac{1}{\sqrt{\Delta_V}} \right\},$$

where  $T$  denotes the total number of triangles, and  $\Delta_V$  and  $\Delta_E$  represent suitable concentration parameters as defined above. With this choice of parameters, the resulting algorithm achieves a space complexity of

$$\mathcal{O}\left(\frac{m}{T} \left(\Delta_E + \sqrt{\Delta_V}\right)\right),$$

and yields an estimator with variance  $\mathcal{O}(T^2)$ .

---

**Algorithm 1**  $T_1$  Estimator (Purely Classical)

---

**Procedure**  $T_1\_Estimator\_Subroutine\_FullyClassical(E; h_E, h_V; p_E, p_V)$

**Input:**  $E$  signed edge stream;  $h_E, h_V$  probabilistic hashes;  $p_E, p_V \in (0, 1]$ .

**Output:** Estimate  $R_1$ .

```

1:  $R_1 \leftarrow 0, S \leftarrow \{\cdot\}$ 
2: for  $(vw, \sigma_{vw}) \in E$ : do
3:   for  $u \in V$ : do
4:     if  $h_V(u) = 1$  and  $uv, uw \in S.keys()$  then            $\triangleright$  Found a triangle, check it is a  $T_1$ 
5:       if  $\sigma_{vw} = +1$  and  $S[uv], S[uw] = -1$  then
6:          $R_1 \leftarrow R_1 + 1/(p_V p_E^2)$ 
7:       else if  $\sigma_{vw} = -1$  and  $S[uv] \neq S[uw]$  then
8:          $R_1 \leftarrow R_1 + 1/(p_V p_E^2)$ 
9:     if  $h_E(vw) = 1$  and  $(h_V(v) = 1$  or  $h_V(w) = 1)$  then
10:       $S[vw] \leftarrow \sigma_{vw}$ 
11: return  $R_1$ 

```

---

Adapting a similar approach for signed edge stream, we consider same sampling probability for vertex and edges which are implemented using probabilistic hash functions denoted as  $h_V$  and  $h_E$  respectively. However, in signed edge stream we have for types of triangle  $T_j$ ,  $j = 0, 1, 2, 3$ . To address the sign of the incoming edges in the stream, we store the edges in the sketch  $S$  with sign. For an incoming edge  $(vw, \sigma_{vw})$ , when a vertex  $u$  is sampled and  $uv, uw \in S$ , we increase the count of the type of triangles  $T_j$  based on  $\sigma_{vw}$  the signs of  $uv$  and  $uw$ . The sketch is updated stochastically to include  $vw$  depending on the probabilities  $h_E(vw)$ ,  $h_V(v)$ , and  $h_V(w)$ . We describe the algorithm for  $j = 1$  in Algorithm 1. Note that our algorithm is an extension of the JK algorithm incorporating the signs of the edges in the stream and hence we call our algorithm signed JK algorithm.

Then we have the following corollary, which gives the bit complexity of space for the algorithm.

**Corollary 1.** *For small error parameters  $\epsilon, \delta > 0$ , there is a median-of-means algorithm for insertion-only graph streams that approximates the number of  $T_1$  triangles in a graph  $G$  to  $\epsilon T_1$  precision with probability  $1 - \delta$ , using*

$$\mathcal{O}\left(\frac{m}{T_1} \left(\Delta_E + \sqrt{\Delta_V}\right) \log n \frac{1}{\epsilon^2} \log \frac{1}{\delta}\right) \quad (5)$$

bits of space. This algorithm uses Alg. 1 as a sub-routine.

As this is a simple signed extension of the JK algorithm, the proof follows almost identically to the proof of Theorem 1.1 in Ref. [8].

#### 4 Hybrid Quantum-Classical Algorithm for Signed Triangle Counting

Here we present the hybrid algorithm for estimating  $T_1$  triangles. A similar approach can be adapted for other types of triangles. The entire framework is split into 2 subroutines that work in parallel as for estimating unsigned triangles [3]. The quantum algorithm that estimates  $T_1^{<k}$  is described in Section 4.2. The classical algorithm that estimates  $T_1^{>k}$  is described in Section 4.1. These are summed to provide an estimate on  $T_1$ , as described in Section 4.3.

##### 4.1 Classical Estimator for $T_1^{>k}$

We extend `ClassicalEstimator` from Ref. [3] to the signed version in the following algorithm.

---

##### Algorithm 2 $T_1^{>k}$ Estimator (Classical)

---

**Procedure:** `T1_Estimator_Classical_Subroutine(E; k; hV, hI)`

**Input:**  $E$  signed edge stream ;  $k \in [1, m]$ ;  $h_V, h_I$  probabilistic hashes.

**Output:** Estimate  $R_1^{>k}$ .

```

1:  $R_1^{>k} \leftarrow 0, S \leftarrow \emptyset, D_- \leftarrow \{:\}, D_+ \leftarrow \{:\}, \ell \leftarrow 0$ 
2: for  $(vw, \sigma_{vw}) \in E$ : do
3:   for  $u \in V$ : do
4:     if  $\sigma_{vw} = +$  then
5:       if  $(u, v, -), (u, w, -) \in S$  then
6:          $R_1^{>k} \leftarrow R_1^{>k} + 1 - (1 - 1/k)^{D_-[(u,v)] + D_+[(u,v)] + D_-[(u,w)] + D_+[(w,v)]}$ 
7:       else
8:         if  $(u, v, +), (u, w, -) \in S$  then
9:            $R_1^{>k} \leftarrow R_1^{>k} + 1 - (1 - 1/k)^{D_-[(u,v)] + D_-[(u,w)] + D_+[(u,w)]}$ 
10:        if  $(u, v, -), (u, w, +) \in S$  then
11:           $R_1^{>k} \leftarrow R_1^{>k} + 1 - (1 - 1/k)^{D_-[(u,v)] + D_+[(u,w)] + D_-[(u,w)]}$ 
12:        for  $(x, y, t) \in S$  do
13:          if  $y \in \{v, w\}$  then
14:            if  $\sigma_{vw} = +1$  then
15:               $D_+[(x, y)] \leftarrow D_+[(x, y)] + 1$ 
16:            else
17:               $D_-[(x, y)] \leftarrow D_-[(x, y)] + 1$ 
18:          if  $h_V(v) = 1$  and  $h_I(\ell) = 1$  then
19:             $S.add((v, w, \sigma_{vw}))$  and set  $D_-[(v, w)], D_+[(v, w)] \leftarrow 0$ .
20:          if  $h_V(w) = 1$  and  $h_I(\ell + 1) = 1$  then
21:             $S.add((w, v, \sigma_{vw}))$  and set  $D_-[(w, v)], D_+[(w, v)] \leftarrow 0$ .
22:           $\ell \leftarrow \ell + 2$ 
23: return  $R_1^{>k}$ 

```

---

The probabilistic hash functions must satisfy  $Pr(h_V(u)) = 1/\sqrt{km}$  and  $Pr(h_I(t)) = \sqrt{k/m}$ .  $h_V$  needs to be stored as it is called multiple times but it can be simplified to being only pairwise independent which requires  $O(\log n)$  bits.  $h_I$  only needs to be queried once and then forgotten, thus we do not need need to store the full function.

**Lemma 2** (Analysis of Alg. 2). (1) *In expectation, the algorithm requires uses  $O(\log n)$  bits to run.*

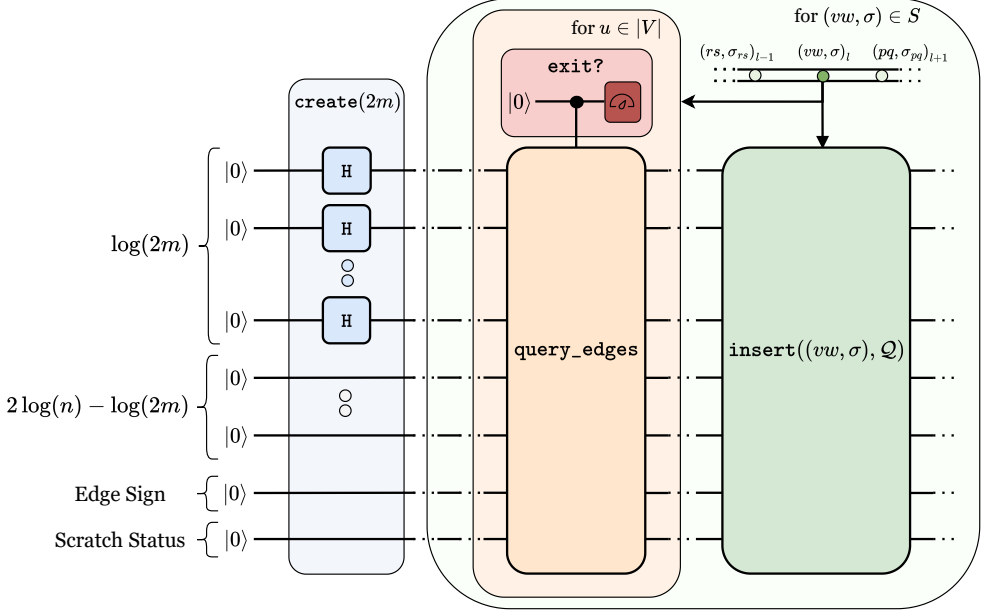


Fig. 3. **Circuit Diagram for Quantum Sketching Algorithm.** The circuit for the quantum sketchpad is described by 3 types of action to update the quantum state as described in Section 4.2. First, create is applied to generate the initial sketchpad, depicted is the case that  $\log(2m)$  is a power of 2 such that Hadamard gates can be used. For each signed edge  $(vw, \sigma)$  in the stream, `query_edges` is applied for every  $u \in |V|$  related to  $vw$  and  $\sigma$ . If one of the PVMs results in a measurement besides  $\perp$ , the algorithm halts and the value is returned. Lastly, `insert` is applied to add  $(vw, \sigma)$  and  $(wv, \sigma)$  to the sketchpad and we proceed to the next edge.

$$(2) \mathbb{E}(R_1^{>k}) = \frac{T_1^{>k} \sqrt{k}}{m^{3/2}}$$

$$(3) \text{Var}(R_1^{>k}) \leq 4 \frac{T_1^{>k} \sqrt{k} \Delta_E}{m^{3/2}}$$

**Corollary 3.** *There is an median-of-means algorithm using Alg. 2 as a subroutine that outputs an estimate of  $T_1^{>k}$  to  $\epsilon T_1$  precision with probability  $1 - \delta$ . This algorithm uses  $\mathcal{O}\left(\frac{m^{3/2}}{T\sqrt{k}} \Delta_E \log n \frac{1}{\epsilon^2} \log \frac{1}{\delta}\right)$  number of classical and quantum bits in expectation.*

The proof of these statements mirrors those of lemmas 8-11 in Ref. [3]. In particular, the only difference is that in lines 5, 8, and 10, we check if there is a  $T_1$  triangle centered on the wedge  $(vw, \sigma_{vw})$ . On line 7 in `ClassicalEstimator` from Ref. [3], they check if there is *any* triangle centered on the wedge  $vw$ . In both cases, once the desired triangle is found, the appropriate value is added to the estimate.

#### 4.2 Quantum Estimator for $T_1^{<k}$

We now use a quantum subroutine to approximate  $T_1^{<k}$ . The subroutine relies on 3 quantum primitives as outlined in Ref. [1]. At a high level, this algorithm records a sketch  $\mathcal{S}$  of seen edges into a quantum state  $\mathcal{Q}_{\mathcal{S}}$  and queries the sketch by measuring  $\mathcal{Q}_{\mathcal{S}}$ . We maintain a state on  $2\lceil \log_2 n \rceil + 2$  qubits, where  $n$  is the number of vertices in the underlying graph. Upon reading a

signed edge  $(vw, \sigma_{vw})$ , a query is made on the underlying sketch for a wedge  $wu, wv$  (along with sign information). This query is done via measurements (see Section C.2 for more details). If no wedge is found, then  $(vw, \sigma_{vw})$  is inserted into the sketch and we proceed to the next edge. It is important to note that this algorithm is *destructive*; processing an edge  $(vw, \sigma_{vw})$  destroys previous information on edges incident to  $v$  and  $w$ . A circuit corresponding to this is depicted in Figure 3.

---

**Algorithm 3**  $T_1^{<k}$  Estimator Subroutine
 

---

**Procedure**  $T_1\_Estimator\_Quantum\_Subroutine(E, k, g)$

**Input:**  $E$  signed edge stream;  $k \in [1, m]$ ;  $g$  probabilistic hash.

**Output:** Estimate  $R_1^{<k}$ .

1:  $Q_S := \text{create}([2m] \times \{\xi\})$ .

2:  $\ell := 0$

3: **for**  $(vw, \sigma_{vw}) \in E$ : **do**

▷ Assume  $v < w$

4:   **if**  $g(\ell) = 1$  **then**

5:     **for**  $u \in V$ : **do**

6:       **if**  $\sigma_{vw} = +$  **then**

7:           $r_{--} := \text{query\_edges}((uv, -), (uw, -), Q)$

8:          **if**  $r_{--} \neq \perp$  **then return**  $r_{--} \cdot km$

9:       **else**

10:           $r_{+-} := \text{query\_edges}((uv, +), (uw, -), Q)$

11:          **if**  $r_{+-} \neq \perp$  **then return**  $r_{+-} \cdot km$

12:           $r_{-+} := \text{query\_edges}((uv, -), (uw, +), Q)$

13:          **if**  $r_{-+} \neq \perp$  **then return**  $r_{-+} \cdot km$

14:      $\text{insert}((vw, s), \ell, Q_S)$

15:      $\ell := \ell + 1$

16: **return** 0

---

In this extension of QuantumEstimator from Ref. [3], we need track of and query for signed edges. Note that the queries in lines 9 and 11 are on disjoint pairs and thus independent.

**Lemma 4** (Performance of Alg. 3). *Let  $R_1^{<k}$  be the outcome of Alg. 3.*

(1) *The algorithm uses  $2 \log(n) + 2 = O(\log n)$  qubits to run.*

(2)  $\mathbb{E}[R_1^{<k}] = T_1^{<k}$ .

(3)  $\text{Var}(R_1^{<k}) \leq (km)^2$ .

The proof of (2) and (3) from this algorithm are given in Section D.

**Corollary 5.** *There is an median-of-means algorithm using Alg. 3 as a subroutine that outputs an estimate of  $T_1^{>k}$  to  $\epsilon T_1$  precision with probability  $1 - \delta$ . This algorithm uses  $O\left(\left(\frac{km}{T_1}\right)^2 \log(n) \frac{1}{\epsilon^2} \log\left(\frac{1}{\delta}\right)\right)$  number of classical and quantum bits in expectation.*

### 4.3 Hybrid Algorithm for $T_1 = T_1^{>k} + T_1^{<k}$

We are now ready to provide the full algorithm that estimates  $T_1$ . Note that this algorithm assumes that one has a reasonable bound on  $m$ ,  $\Delta_E$ , and  $T_1$  itself. This is an almost identical statement and proof to Theorem 1 in Ref. [3].

**THEOREM 6.** *For any  $\epsilon, \delta \in (0, 1]$ , there is a hybrid quantum-classical streaming algorithm that uses*

$$O\left(\frac{m^{8/5}}{T_1^{6/5}} \Delta_E^{4/5} \log n \cdot \frac{1}{\epsilon^2} \log \frac{1}{\delta}\right) \quad (6)$$

*quantum and classical bits in expectation to return a  $(1 \pm \epsilon)$ -multiplicative approximation of  $T_1$  in an insertion-only graph stream with probability  $1 - \delta$ .*

**PROOF.** Let `T1_Estimator_Classical` and `T1_Estimator_Quantum` be the names of the median-of-means algorithms promised by Corollaries 3 and 5. The following algorithm achieves the performance of the theorem. Lines 2 and 3 are written sequentially but should really be run in parallel.

---

**Algorithm 4** Signed  $T_1$  Estimator (Quantum-Classical)

---

**Procedure** `T1_Estimator_Hybrid(E,  $\epsilon, \delta$ )`

**Input:**  $E$  stream of  $m$  signed edges;  $\epsilon, \delta$  error params.

**Output:** Estimate  $R_1$ .

1:  $k \leftarrow \left\lceil \frac{(T_1)^{2/5} (\Delta_E)^{2/5}}{m^{1/5}} \right\rceil$

Run the following sub-routines in parallel:

2:  $R_1^{>k} \leftarrow \text{T}_1\text{-Estimator\_Classical}(E, k, \epsilon/2, \delta/2)$

3:  $R_1^{<k} \leftarrow \text{T}_1\text{-Estimator\_Quantum}(E, k, \epsilon/2, \delta/2)$

4: **return**  $R_1^{>k} + R_1^{<k}$

---

To show accuracy, recall that  $R_1^{>k}$  is an estimate of  $T_1^{>k}$  up to  $\epsilon T_1/2$  precision with probability  $1 - \delta/2$ . Similarly,  $R_1^{<k}$  is an estimate of  $T_1^{<k}$  up to  $\epsilon T_1/2$  precision with probability  $1 - \delta/2$ . Then  $R_1 = R_1^{>k} + R_1^{<k}$  is an estimate of  $T_1 = T_1^{<k} + T_1^{>k}$  to precision  $\epsilon T_1$  with probability  $1 - \delta$  via a union bound.

As for the space required, note that the estimates of  $R_1^{>k}$  and  $R_1^{<k}$  require  $\tilde{O}\left(\frac{m^{3/2}}{T_1 \sqrt{k}} \Delta_E\right)$  and  $\tilde{O}\left(\left(\frac{km}{T_1}\right)^2\right)$  space, respectively, ignoring the common log terms. When  $k = \left\lceil \frac{(T_1)^{2/5} (\Delta_E)^{2/5}}{m^{1/5}} \right\rceil$ , these both become  $\tilde{O}\left(\frac{m^{8/5}}{T_1^{6/5}} \Delta_E^{4/5}\right)$ .  $\square$

Lastly, we would like to compare the space used by the hybrid algorithm Alg. 4 versus its classical counterpart Alg. 1. As noted in Ref. [3], the graph parameters that maximize the separation are  $\Delta_E = O(1)$  and  $\Delta_V = \Omega(T_1) = \Omega(m)$ , resulting in a  $\tilde{O}(m^{2/5})$ -space hybrid algorithm versus  $\Omega(\sqrt{m})$ -space purely classical algorithm. This is also true in our setting.

## 5 A distributed quantum-classical computing model for estimating balance of signed graphs

In this section, we estimate the triangular index of balance of signed graphs using the streaming algorithms developed in the previous section. In order to estimate the balance with accuracy  $(1 \pm \epsilon)$ -multiplicative approximation with probability  $1 - \delta$  we estimate the counts of triangle types  $T_j$  with accuracy  $(1 \pm \epsilon/(2 + \epsilon))$ -multiplicative approximation with probability  $1 - \delta$ . Using a simple algebraic manipulation it can be justified. Then we discuss a quantum distributed model for implementation of our proposed quantum-classical algorithm for estimating balance.

### 5.1 Algorithm for Estimating Triangular Balance

We now use the individual triangle estimators to construct an algorithm that estimates triangle balance (Eq. (4)).

**Corollary 7.** *For any  $\epsilon, \delta \in (0, 1]$ , there is a hybrid quantum-classical streaming algorithm that uses*

$$\mathcal{O}\left(\frac{m^{8/5}}{T^{6/5}} \Delta_E^{4/5} \log n \cdot \frac{1}{\epsilon^2} \log \frac{1}{\delta}\right) \quad (7)$$

*quantum and classical bits in expectation to return a  $(1 \pm \epsilon)$ -multiplicative approximation of  $\mathcal{B}_\Delta(G)$  in an insertion-only graph stream with probability  $1 - \delta$ .*

Let `T_Estimator_Hybrid` be the algorithm described by Lemma 11 in Ref. [3].

---

#### Algorithm 5 Balance Estimator (Hybrid)

---

**Procedure** `BalanceEstimator_Hybrid`( $E, \epsilon, \delta$ )

**Input:**  $S$  signed edge stream;  $\epsilon, \delta \in (0, 1]$  error params.

**Output:** Estimate  $\overline{\mathcal{B}}_\Delta^H(G)$ .

Run the following sub-routines in parallel:

- 1:  $R_1 \leftarrow \text{T\_Estimator\_Hybrid}(S, \epsilon/(2 + \epsilon), \delta/3)$
  - 2:  $R_3 \leftarrow \text{T\_Estimator\_Hybrid}(S, \epsilon/(2 + \epsilon), \delta/3)$  ▷ Dropping  $-1$  edges
  - 3:  $R \leftarrow \text{T\_Estimator\_Hybrid}(S, \epsilon/(2 + \epsilon), \delta/3)$  ▷ Ignoring signs
  - 4: **return**  $(R_1 + R_3)/R$
- 

As a comparison to the hybrid algorithm, we also use a purely classical algorithm to estimate  $\mathcal{B}_\Delta(G)$ . This is a slight variation to Alg. 1.

**Algorithm 6** Balance Estimator (Purely Classical)**Procedure** Bal\_Estimator\_Subroutine\_FullyClassical( $E; h_E, h_V; p_E, p_V$ )**Input:**  $E$  signed edge stream;  $h_E, h_V$  probabilistic hashes;  $p_E, p_V \in (0, 1]$ .**Output:** Estimate  $\overline{\mathcal{B}}_\Delta^C(G)$ .

```

1:  $R_{bal}, R_{unbal} \leftarrow 0, S \leftarrow \{:\}$ 
2: for  $(vw, \sigma_{vw}) \in E$ : do
3:   for  $u \in V$ : do
4:     if  $h_V(u) = 1$  and  $uw, uv \in S.keys()$  then     $\triangleright$  Found a triangle, check for correct type
5:       if  $\sigma_{vw} = +$  then
6:         if  $(S[uv], S[uw]) = -1$  or  $(S[uv], S[uw]) = +1$  then
7:            $R_{bal} \leftarrow R_{bal} + 1/(p_V p_E^2)$            $\triangleright$  Triangle type  $T_1$  or  $T_3$ 
8:         else
9:            $R_{unbal} \leftarrow R_{unbal} + 1/(p_V p_E^2)$      $\triangleright$  Triangle type  $T_0$  or  $T_2$ 
10:        else
11:          if  $(S[uv], S[uw]) = -1$  or  $(S[uv], S[uw]) = +1$  then
12:             $R_{unbal} \leftarrow R_{unbal} + 1/(p_V p_E^2)$    $\triangleright$  Triangle type  $T_0$  or  $T_2$ 
13:          else
14:             $R_{bal} \leftarrow R_{bal} + 1/(p_V p_E^2)$        $\triangleright$  Triangle type  $T_1$  or  $T_3$ 
15:        if  $h_E(vw) = 1$  and  $(h_V(v) = 1$  or  $h_V(w) = 1)$  then
16:           $S[vw] \leftarrow \sigma_{vw}$ 
17: return  $R_{bal}/(R_{bal} + R_{unbal})$ 

```

**Conjecture 8.** *There is a polynomial space advantage to the hybrid quantum-classical triangle balance algorithm compared with state-of-the-art purely classical estimators.*

The motivation for the conjecture is that the hybrid algorithm is composed of 3 subroutines all with space advantage over their purely-classical counterparts. However, it is not clear if there is a better purely-classical algorithm to estimate balance that does not rely on explicitly calculating balanced and unbalanced triangles.

## 5.2 The Distributed Computing Setup

We now propose a distributed computing framework to implement the hybrid algorithm. Recall that distributed quantum computing (DQC) aims to scale quantum computation by leveraging quantum and/or classical communication links among multiple quantum devices [46]. A central challenge in standard DQC architectures is the realization of distributed quantum operations, such as quantum gates acting across different devices. In contrast, our framework does not require any distributed quantum operations. Instead, each small quantum device operates independently, and the resulting classical outputs are communicated to a classical processor for post-processing to obtain the final estimate. This structure renders the proposed algorithm *perfectly distributable* in the sense of Ref. [24]. Our approach is a form of embarrassingly parallelizable MapReduce paradigm, as depicted in Figure 4. In the following, we describe the quantum and classical resources required and detail the implementation of the hybrid algorithm within this distributed setting.

**5.2.1 Computational resources and procedure.** For a fixed sign graph  $G$  on  $n$  vertices, let  $\mathcal{B}_\Delta$  denote the true triangular balance. Then given  $0 < \epsilon, \delta < 1$  the hybrid algorithm estimates  $\mathcal{B}_\Delta$  with precision  $\epsilon \mathcal{B}_\Delta$  with probability  $1 - \delta$ . Fix constants  $N_Q = \Theta((km/T\epsilon)^2 \log \frac{1}{\delta})$  and  $N_C =$

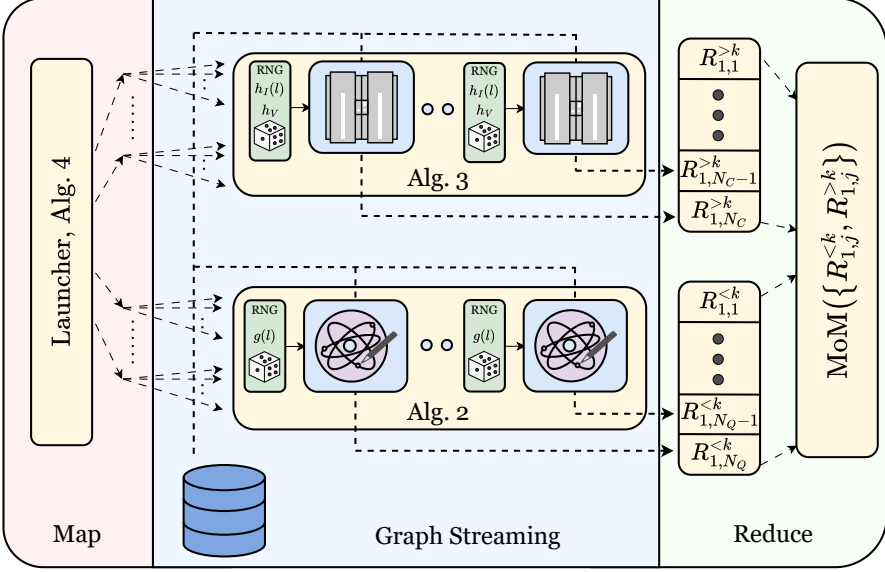


Fig. 4. **A Schematic for Signed Triangle Estimation with Distributed Resources.** During the *mapping*, based on Alg. 4, we allocate QPUs and CPUs with their respective initial (empty) sketchpads. During the *Graph Streaming*, each edge is passed to these distributed CPUs and QPUs. At step  $\ell$  in the stream, based on the hash functions  $g(\ell)$ ,  $h_I(\ell)$  and  $h_V$ , each CPU or QPU applies a query (see Figure 3). Each CPU and QPU will terminate asynchronously and provide their estimate. During the *reduction*, we calculate the median-of-means (MoM in diagram) based on parameters  $\delta$  and  $\epsilon$ .

$\Theta\left(\frac{m^{3/2}\Delta_E}{T\sqrt{k}\epsilon^2} \log \frac{1}{\delta}\right)$ . The DC setup requires  $3N_Q$  small-scale QPUs and  $3N_C$  CPUs. Here  $m$  is an approximate number of edges in the stream,  $T$  is the approximate number of triangles in  $G$ , and  $k \approx T^{2/5}\Delta_E^{2/5}/m^{1/5}$ .

- (1) **Quantum resources:** Each QPU is supported with a classical register that implements the hash function  $h_E$  independently for each incoming edge  $e$  such that  $h_E(e) = 1$  with probability  $1/k$  and 0 otherwise. There is a  $(2\lceil\log_2 n\rceil + 2)$ -qubit quantum register, which implements the sketchpad. Indeed, the working qubit register is formed by  $2\lceil\log_2 n\rceil$  qubits, and there are two one-qubit registers used for scratch-qubit and the last one stores the sign of an incoming edge in the stream. Each QPU is also supported by a measurement device which performs queries to the quantum sketchpad as described by Algorithm 3.
- (2) **Classical resources:** Each CPU is supported by a hash function  $h_V$  such that  $\mathbb{E}[h_V(u)] = 1/\sqrt{km}$  for each vertex  $u$  of  $G$ . In addition, it is associated with a sketchpad memory register which stores an incoming signed edge and probabilistically updated as described by Algorithm 2.

Now we discuss the working procedure of the distributed computing setup as illustrated by a schematic diagram in Figure 4. The overall procedure approximates three values in parallel:  $R_1$ ,  $R_3$ , and  $R$ . By outputting  $(R_1 + R_3)/R$ , we get an approximation of  $\mathcal{B}_\Delta$ .

A central classical organizer is in charge of by preparing  $3N_Q$  QPUs and  $3N_C$  CPUs. Each of these requires their own independent randomness and is in charge of calculating an estimate for one of the three values above. Roughly speaking,  $N_Q$  QPUs and  $N_C$  CPUs contribute to the approximation

of  $R_1$ ,  $N_Q$  QPUs and  $N_C$  CPUs contribute to the approximation of  $R_3$ , and  $N_Q$  QPUs and  $N_C$  CPUs contribute to the approximation of  $R$ . As edges are streamed, they are broadcast to every processor (quantum and classical) simultaneously. Once all the devices (quantum and classical) are done, they report their values to the central processor where classical Median-of-Means post-processing is performed to obtain the three individual estimates.

To make this process more precise, we focus on the  $R_1$  approximation (see Figure 4). For each  $j \in [N_C]$ , a CPU independently produces  $R_{1,j}^{>k}$  which is returned to the central organizer. Let  $N_{C,\epsilon} := \frac{m^{3/2}\Delta E}{T_1\sqrt{k\epsilon^2}}$  and  $N_{C,\delta} := \log \frac{1}{\delta}$  such that  $N_C = N_{C,\epsilon} \cdot N_{C,\delta}$ . We bucket the first  $N_{C,\epsilon}$  values to compute

$$\widehat{R_{1,1}^{>k}} := \text{mean} \left( R_{1,1}^{>k}, \dots, R_{1,N_{C,\epsilon}}^{>k} \right). \quad (8)$$

Next, compute  $\widehat{R_{1,2}^{>k}}$  by bucketing and taking the mean of the next  $N_{C,\epsilon}$  values  $\left\{ R_{1,N_{C,\epsilon}+1}^{>k}, \dots, R_{1,2N_{C,\epsilon}}^{>k} \right\}$ .

Proceed until we have averages  $\widehat{R_{1,1}^{>k}}, \dots, \widehat{R_{1,N_{C,\delta}}^{>k}}$ . From here, we attain the final classical estimate of  $T_1^{>k}$  as

$$R_1^{>k} := \text{median} \left( \widehat{R_{1,1}^{>k}}, \dots, \widehat{R_{1,N_{C,\delta}}^{>k}} \right). \quad (9)$$

$R_1^{>k}$  is then a good estimator for  $T_1^{>k}$ .

A similar post-processing is done with the quantum outputs. First, divide the  $N_Q$  QPUs in charge of estimating  $R_1^{<k}$  into  $N_{Q,\epsilon} := (km/T_1\epsilon)^2$  buckets, each producing an average  $\widehat{R_{1,j}^{<k}}$  for  $j \in [N_{Q,\delta}]$ , where  $N_{Q,\delta} := \log \frac{1}{\delta}$ . Take the median of these values to produce  $R_1^{<k}$  which is an estimate of  $T_1^{<k}$ . By summing  $R_1^{>k}$  and  $R_1^{<k}$ , we obtain a good estimate of  $T_1$ . This same process is repeated in parallel to obtain estimates of  $R_3$  and  $R$ . To finish, we output  $(R_1 + R_3)/R$  to achieve an estimate  $\overline{\mathcal{B}}_\Delta^H$  of  $\mathcal{B}_\Delta$ .

### 5.3 Numerical Simulations

**5.3.1 Simulating the Quantum Sketchpad.** In order to test the hybrid algorithm Alg. 5 on real graphs, we need to implement the quantum operations. The space required for any non-trivial example is much too large to be run on current devices so this process is simulated. This is done by a classical sketch whose operations obey the probabilities described in the Section 4.2. In particular, the simulated sketch has the three methods `create`, `insert`, `query_edges` that mimics the probabilistic behavior of the quantum sketch. See Section A for the code implementation.

**5.3.2 Results.** We run Algs. 5 and 6 on a set of Erdős–Rényi graphs that additionally have randomly assigned edge signs. These graphs were created with two probabilities: the edge probability  $p_e$  and for each edge, the probability that the sign is positive  $p_+$ . For each tuple of parameters  $(n, p_e, p_+) \in \{10, 20, 30, 40, 50\} \times \{0.5, 0.75\} \times \{0.25, 0.5, 0.75\}$ , 5 random graphs were created. Tables 1 to 3 shows the  $n \in \{30, 40, 50\}$  instances generated and used in these experiments. For conciseness, the  $n \in \{10, 20\}$  instances are omitted but the algorithms' performances are similar to the larger graph sizes.

Each algorithm was run with error parameters  $\epsilon, \delta = 0.1$ . For a fixed graph, let  $\overline{\mathcal{B}}_\Delta^H$  and  $\overline{\mathcal{B}}_\Delta^C$  be the outputs of Algs. 5 and 6, respectively, and  $\mathcal{B}_\Delta$  the true value. Then using these parameters, both  $\overline{\mathcal{B}}_\Delta^H$  and  $\overline{\mathcal{B}}_\Delta^C$  approximate the  $\mathcal{B}_\Delta$  up to  $0.1\mathcal{B}_\Delta$  accuracy with probability at least 0.9. As can be seen in Figure 5, both estimators outperform the  $\epsilon = 0.1$  error threshold. Moreover, the hybrid algorithm performs moderately outperforms the purely-classical signed JK algorithm.

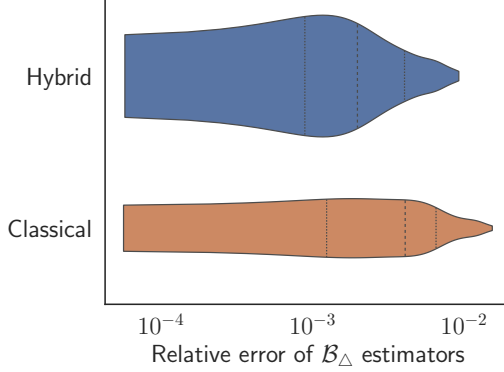


Fig. 5. **Violin Plot Comparing the Performance of Classical and Quantum-Classical Triangular Balance Estimators.** Comparison between  $\overline{\mathcal{B}}_{\Delta}^H$  and  $\overline{\mathcal{B}}_{\Delta}^C$  outputted by Alg. 5 versus Alg. 6, respectively. These algorithms are tested over random Erdős–Rényi instances of sizes  $n \in \{30, 40, 50\}$ . The relative error is computed as  $|\overline{\mathcal{B}}_{\Delta}^A - \mathcal{B}_{\Delta}|/\mathcal{B}_{\Delta}$  for  $A \in \{H, C\}$ . Both algorithms are ran with accuracy parameter  $\epsilon = 0.1$  and the performance is better than expected. The hybrid algorithm slightly outperforming the purely classical but does experience higher variance. This is to be expected, as there are two sources of error for the hybrid algorithm, one from the quantum and one from the classical estimators.

## 6 Conclusion

In this manuscript, we delineate a natural extension of the space-optimal classical algorithm for counting unsigned triangles into the signed case, where we need to count the four different types of signed triangles that can appear in a signed network stream. We then delineate a hybrid quantum-classical algorithm that provides a polynomial space advantage over the classical algorithm.

Approximately counting the different types of triangles in a signed network has been tied to many kinds of important real-life network dynamics, through the lens of structural balance theory. In particular, we consider the task of estimating the balance of a sign network, tied to understanding conflict or discord in social networks, financial markets, biological systems, and more.

Our work shows that quantum computers can be utilized in the monitoring and interpretation of large scale networks, achieving quantum advantage over the best possible classical algorithm for estimating central parameters such as balance.

## References

- [1] J. Kallaugher, O. Parekh, and N. Voronova, “How to design a quantum streaming algorithm without knowing anything about quantum computing,” Oct. 2024, arXiv:2410.18922.
- [2] D. Gavinsky, J. Kempe, and R. d. Wolf, “Exponential separation of quantum and classical one-way communication complexity for a boolean function,” Jul. 2006, arXiv:quant-ph/0607174.
- [3] J. Kallaugher, “A quantum advantage for a natural streaming problem,” in *2021 IEEE 62nd Annual Symposium on Foundations of Computer Science (FOCS)*. IEEE, 2022, pp. 897–908.
- [4] J. Kallaugher, O. Parekh, and N. Voronova, “Exponential quantum space advantage for approximating maximum directed cut in the streaming model,” Nov. 2023, arXiv:2311.14123.
- [5] Z. Bar-Yossef, R. Kumar, and D. Sivakumar, “Counting triangles in data streams,” in *Proceedings of the 21st ACM SIGMOD-SIGACT-SIGAI Symposium on Principles of Database Systems (PODS)*. ACM, 2002, pp. 134–141.
- [6] L. S. Buriol, G. Frahling, S. Leonardi, A. Marchetti-Spaccamela, and C. Sohler, “Counting triangles in data streams,” in *Proceedings of the 25th ACM SIGMOD-SIGACT-SIGAI Symposium on Principles of Database Systems (PODS)*. ACM, 2006, pp. 253–262.

Table 1. **Numerical Results for Signed Erdős–Rényi Graphs with  $n = 30$  Nodes.** A bolded value corresponds to that estimate being closer to the true value  $\mathcal{B}_\Delta = (T_1 + T_3)/\sum_i T_i$ . In this table, the  $\overline{\mathcal{B}}_\Delta^A$  values are truncated to three decimals here for compactness and so it may appear that they are equivalent for some rows.

$p_E$	$p_+$	$E_+$	$E_-$	$\Delta_E$	$\Delta_V$	$T_0$	$T_1$	$T_2$	$T_3$	$\mathcal{B}_\Delta$	$\overline{\mathcal{B}}_\Delta^C$	$\overline{\mathcal{B}}_\Delta^H$
0.75	0.5	148	171	21	233	215	676	557	147	0.516	0.513	<b>0.517</b>
0.75	0.25	75	260	23	255	852	768	202	19	0.427	0.428	<b>0.428</b>
0.5	0.25	42	156	13	79	185	165	26	5	0.446	0.445	<b>0.445</b>
0.75	0.5	150	195	23	255	355	861	633	158	0.508	0.506	<b>0.508</b>
0.5	0.5	108	111	13	101	72	199	196	61	0.492	<b>0.492</b>	0.492
0.5	0.5	107	116	12	86	70	224	176	53	0.530	0.523	<b>0.530</b>
0.5	0.25	62	161	14	104	221	261	77	14	0.480	<b>0.479</b>	0.479
0.75	0.5	171	161	24	271	189	661	730	239	0.495	0.497	<b>0.494</b>
0.5	0.25	51	164	12	80	221	202	63	5	0.422	0.420	<b>0.421</b>
0.75	0.25	79	239	20	218	697	648	221	26	0.423	0.427	<b>0.427</b>
0.5	0.5	101	110	12	86	71	174	171	53	0.484	0.481	<b>0.482</b>
0.75	0.5	152	165	21	215	201	612	561	195	0.514	<b>0.514</b>	0.512
0.5	0.5	94	114	12	72	63	173	138	42	0.517	0.522	<b>0.520</b>
0.75	0.75	247	71	22	237	22	187	631	765	0.593	<b>0.593</b>	0.593
0.5	0.25	50	168	15	103	230	241	57	10	0.467	0.472	<b>0.464</b>
0.5	0.75	163	64	14	106	15	90	262	211	0.521	0.518	<b>0.523</b>
0.5	0.75	150	57	11	70	10	86	167	164	0.585	0.585	<b>0.585</b>
0.5	0.25	45	151	11	68	172	132	45	3	0.384	0.387	<b>0.386</b>
0.75	0.25	100	233	24	267	632	795	345	51	0.464	0.468	<b>0.465</b>
0.5	0.75	166	51	12	84	5	61	202	217	0.573	0.566	<b>0.570</b>
0.75	0.75	254	78	23	284	28	257	689	813	0.599	<b>0.599</b>	0.598
0.75	0.75	224	92	21	228	37	290	672	546	0.541	0.534	<b>0.543</b>
0.75	0.5	170	137	20	240	122	470	569	248	0.510	0.513	<b>0.508</b>
0.5	0.75	147	54	12	75	4	66	182	142	0.528	0.525	<b>0.529</b>
0.75	0.75	255	76	22	247	22	226	720	816	0.584	0.587	<b>0.583</b>
0.75	0.25	95	223	20	214	520	702	301	36	0.473	<b>0.474</b>	0.470
0.75	0.75	255	76	23	263	23	217	739	819	0.576	0.572	<b>0.574</b>
0.5	0.5	97	125	14	94	94	221	192	46	0.483	<b>0.483</b>	0.483
0.75	0.25	87	244	23	245	719	799	264	23	0.455	0.456	<b>0.456</b>
0.5	0.75	161	63	14	96	10	91	238	211	0.549	0.546	<b>0.549</b>

- [7] M. Jha, C. Seshadhri, and A. Pinar, “A space efficient streaming algorithm for estimating transitivity and triangle counts using the birthday paradox,” in *ACM Transactions on Knowledge Discovery from Data*, vol. 9, no. 4, 2015, pp. 1–21.
- [8] R. Jayaram and J. Kallaugher, “Optimal algorithms for counting triangles in graph streams,” in *Proceedings of the 53rd Annual ACM SIGACT Symposium on Theory of Computing (STOC)*. ACM, 2021, pp. 1283–1296.
- [9] J. Leskovec, D. Huttenlocher, and J. Kleinberg, “Signed networks in social media,” in *Proceedings of the SIGCHI Conference on Human Factors in Computing Systems*, 2010, pp. 1361–1370.
- [10] G. Facchetti, G. Iacono, and C. Altafini, “Computing global structural balance in large-scale signed social networks,” *Proceedings of the National Academy of Sciences*, vol. 108, no. 52, pp. 20 953–20 958, 2011.
- [11] T. Antal, P. Kravivsky, and S. Redner, “Dynamics of social balance on networks,” *Physical Review E*, vol. 72, no. 3, p. 036121, 2005.

Table 2. **Numerical Results for Signed Erdős–Rényi Graphs with  $n = 40$  Nodes.** A bolded value corresponds to that estimate being closer to the true value  $\mathcal{B}_\Delta = (T_1 + T_3)/\sum_i T_i$ . In this table, the  $\overline{\mathcal{B}}_\Delta^A$  values are truncated to three decimals here for compactness and so it may appear that they are equivalent for some rows.

$p_E$	$p_+$	$E_+$	$E_-$	$\Delta_E$	$\Delta_V$	$T_0$	$T_1$	$T_2$	$T_3$	$\mathcal{B}_\Delta$	$\overline{\mathcal{B}}_\Delta^C$	$\overline{\mathcal{B}}_\Delta^H$
0.5	0.25	114	297	18	189	549	636	240	23	0.455	<b>0.453</b>	0.459
0.75	0.75	443	156	31	480	74	669	1901	1810	0.557	<b>0.557</b>	0.560
0.75	0.5	284	306	30	450	602	1641	1513	505	0.504	0.505	<b>0.503</b>
0.75	0.5	301	298	30	455	530	1681	1694	562	0.502	0.503	<b>0.503</b>
0.5	0.75	315	73	17	151	6	99	436	667	0.634	<b>0.635</b>	0.637
0.5	0.75	274	104	16	156	19	204	475	424	0.560	<b>0.560</b>	0.563
0.5	0.25	98	311	17	171	631	584	176	19	0.428	0.429	<b>0.429</b>
0.5	0.25	99	287	16	145	520	479	176	23	0.419	0.421	<b>0.419</b>
0.75	0.75	443	147	29	443	60	597	1796	1778	0.561	0.559	<b>0.561</b>
0.75	0.5	293	286	30	439	503	1522	1460	543	0.513	<b>0.512</b>	0.513
0.75	0.25	123	450	29	431	1898	1562	424	44	0.409	0.407	<b>0.408</b>
0.5	0.5	217	199	18	177	168	508	583	193	0.483	0.481	<b>0.482</b>
0.75	0.5	300	285	30	418	483	1502	1617	565	0.496	0.499	<b>0.496</b>
0.75	0.75	440	138	29	395	39	528	1677	1716	0.567	0.568	<b>0.566</b>
0.75	0.25	134	425	29	445	1587	1553	442	56	0.442	0.438	<b>0.444</b>
0.75	0.25	155	428	28	424	1625	1789	656	82	0.451	0.454	<b>0.448</b>
0.75	0.75	466	130	30	436	36	487	1775	2134	0.591	<b>0.591</b>	0.591
0.5	0.5	186	198	18	166	167	416	458	129	0.466	<b>0.466</b>	0.465
0.5	0.25	87	290	17	172	519	470	142	12	0.422	0.424	<b>0.424</b>
0.5	0.75	282	102	17	160	17	180	521	448	0.539	0.544	<b>0.542</b>
0.5	0.75	297	109	18	171	27	226	586	590	0.571	0.573	<b>0.570</b>
0.5	0.5	189	208	18	160	172	506	476	128	0.495	<b>0.493</b>	0.496
0.75	0.25	148	423	29	439	1584	1636	585	64	0.439	0.436	<b>0.438</b>
0.5	0.25	92	317	19	200	644	576	174	19	0.421	0.419	<b>0.421</b>
0.75	0.75	441	144	29	421	59	581	1743	1760	0.565	0.567	<b>0.564</b>
0.5	0.5	197	195	16	167	159	465	485	150	0.488	<b>0.489</b>	0.493
0.75	0.5	306	282	30	426	445	1545	1637	611	0.509	<b>0.509</b>	0.507
0.75	0.25	164	421	29	440	1528	1796	719	96	0.457	0.460	<b>0.457</b>
0.5	0.5	204	186	20	189	141	412	501	175	0.478	<b>0.478</b>	0.477
0.5	0.75	291	94	15	130	14	141	504	514	0.558	0.561	<b>0.556</b>

[12] S. Marvel, S. Strogatz, and J. Kleinberg, “Energy landscape of social balance,” *Physical Review Letters*, vol. 103, no. 19, p. 198701, 2009.

[13] V. Boginski, S. Butenko, and P. Pardalos, “Statistical analysis of financial networks,” *Computational Statistics & Data Analysis*, vol. 48, no. 2, pp. 431–443, 2005.

[14] D. Kenett, M. Tumminello, A. Madi, G. Gur-Gershgoren, R. Mantegna, and E. Ben-Jacob, “Dominating clasp of the financial sector revealed by partial correlation analysis of the stock market,” *PLOS ONE*, vol. 5, no. 12, p. e15032, 2010.

[15] L. Bargigli, G. di Iasio, L. Infante, F. Lillo, and F. Pierobon, “The multiplex structure of interbank networks,” *Quantitative Finance*, vol. 15, no. 4, pp. 673–691, 2015.

[16] P. Bartesaghi, F. Diaz-Diaz, R. Grassi, and P. Uberti, “Global balance and systemic risk in financial correlation networks,” *Physica A: Statistical Mechanics and its Applications*, p. 130698, 2025.

[17] B. Adhikari, “Signed network models for portfolio optimization,” *arXiv preprint arXiv:2510.05377*, 2025.

Table 3. **Numerical Results for Signed Erdős–Rényi Graphs with  $n = 50$  Nodes.** A bolded value corresponds to that estimate being closer to the true value  $\mathcal{B}_\Delta = (T_1 + T_3)/\sum_i T_i$ . In this table, the  $\overline{\mathcal{B}}_\Delta^A$  values are truncated to three decimals here for compactness and so it may appear that they are equivalent for some rows.

$p_E$	$p_+$	$E_+$	$E_-$	$\Delta_E$	$\Delta_V$	$T_0$	$T_1$	$T_2$	$T_3$	$\mathcal{B}_\Delta$	$\overline{\mathcal{B}}_\Delta^C$	$\overline{\mathcal{B}}_\Delta^H$
0.75	0.5	453	479	37	683	1251	3250	3184	957	0.487	<b>0.487</b>	0.487
0.5	0.5	301	297	21	229	271	819	894	304	0.491	0.494	<b>0.494</b>
0.5	0.25	137	438	21	245	887	838	236	31	0.436	<b>0.438</b>	0.438
0.5	0.75	444	160	20	217	39	348	1018	905	0.542	0.539	<b>0.543</b>
0.75	0.5	453	460	37	669	1063	3020	3008	975	0.495	<b>0.493</b>	0.499
0.5	0.25	152	456	22	232	988	1012	335	45	0.444	0.451	<b>0.444</b>
0.75	0.25	222	697	35	610	3580	3447	1080	116	0.433	0.428	<b>0.435</b>
0.75	0.5	441	473	33	610	1127	3191	2854	927	0.508	0.511	<b>0.510</b>
0.5	0.5	313	310	21	221	281	986	961	315	0.512	0.515	<b>0.509</b>
0.75	0.5	452	462	37	666	1034	3093	3039	925	0.497	0.502	<b>0.496</b>
0.5	0.75	455	154	22	261	19	354	1041	981	0.557	0.558	<b>0.557</b>
0.5	0.5	275	353	21	260	473	1104	839	220	0.502	0.505	<b>0.504</b>
0.75	0.25	234	689	34	648	3462	3519	1160	152	0.443	0.442	<b>0.443</b>
0.75	0.75	661	226	33	598	147	1038	3126	3120	0.560	<b>0.559</b>	0.559
0.75	0.25	229	703	39	726	3684	3615	1195	108	0.433	0.429	<b>0.434</b>
0.5	0.5	304	320	21	213	343	952	980	295	0.485	0.485	<b>0.485</b>
0.5	0.25	148	455	21	234	1021	995	311	37	0.437	0.443	<b>0.435</b>
0.75	0.5	449	472	37	706	1105	3179	3017	1001	0.503	<b>0.506</b>	0.508
0.5	0.75	435	164	23	286	47	413	1023	893	0.550	<b>0.550</b>	0.547
0.5	0.5	312	320	24	296	378	982	962	339	0.496	0.496	<b>0.496</b>
0.5	0.75	450	153	20	225	37	328	1012	973	0.554	0.556	<b>0.555</b>
0.5	0.25	134	466	21	220	1067	928	246	23	0.420	0.416	<b>0.419</b>
0.75	0.25	238	665	36	647	3191	3331	1202	142	0.442	0.444	<b>0.441</b>
0.5	0.25	155	457	20	252	1019	1017	336	39	0.438	0.438	<b>0.438</b>
0.75	0.25	230	684	39	731	3429	3433	1192	126	0.435	0.436	<b>0.435</b>
0.75	0.75	664	228	36	654	130	1091	3299	3075	0.549	0.549	<b>0.549</b>

- [18] —, “Signed network models for dimensionality reduction of portfolio optimization,” *arXiv preprint arXiv:2602.21362*, 2026.
- [19] E. Estrada, “Balance in signed biological networks,” *Journal of Theoretical Biology*, vol. 263, no. 4, pp. 556–561, 2010.
- [20] A. Saade, F. Krzakala, and L. Zdeborová, “Spectral clustering of signed networks,” in *Advances in Neural Information Processing Systems (NeurIPS)*, 2014, pp. 1–9.
- [21] C. Altafini, “Consensus problems on networks with antagonistic interactions,” *IEEE Transactions on Automatic Control*, vol. 58, no. 4, pp. 935–946, 2013.
- [22] V. Traag, P. Van Dooren, and P. De Leenheer, “Dynamical models explaining social balance and evolution of cooperation,” *PLOS ONE*, vol. 8, no. 4, p. e60063, 2013.
- [23] L. Meng, Y. Shao, L. Yuan, L. Lai, P. Cheng, X. Li, W. Yu, W. Zhang, X. Lin, and J. Zhou, “A survey of distributed graph algorithms on massive graphs,” *ACM Computing Surveys*, vol. 57, no. 2, pp. 1–39, 2024.
- [24] M. Caleffi, M. Amoretti, D. Ferrari, J. Illiano, A. Manzalini, and A. S. Cacciapuoti, “Distributed quantum computing: a survey,” *Computer Networks*, vol. 254, p. 110672, 2024.
- [25] K. J. Ahn, S. Guha, and A. McGregor, “Graph sketches: Sparsification, spanners, and subgraphs,” in *Proceedings of the 31st ACM SIGMOD-SIGACT-SIGAI Symposium on Principles of Database Systems (PODS)*. ACM, 2012, pp. 5–14.
- [26] A. McGregor, “Graph stream algorithms: A survey,” *SIGMOD Record*, vol. 43, no. 1, pp. 9–20, 2014.

- [27] M. Kapralov, “Streaming algorithms for matching in general graphs,” in *Proceedings of the 24th Annual ACM-SIAM Symposium on Discrete Algorithms (SODA)*. SIAM, 2013, pp. 167–183.
- [28] G. Cormode and S. Muthukrishnan, “Counting triangles and the curse of the last reducer,” in *Proceedings of the 20th International World Wide Web Conference (WWW)*, 2010, pp. 607–614.
- [29] D. P. Woodruff, “Sketching as a tool for numerical linear algebra,” *Foundations and Trends in Theoretical Computer Science*, vol. 10, no. 1–2, pp. 1–157, 2014.
- [30] S. Muthukrishnan, *Data Streams: Algorithms and Applications*. Now Publishers, 2005.
- [31] G. Malewicz, M. H. Austern, A. J. Bik, J. C. Dehnert, I. Horn, N. Leiser, and G. Czajkowski, “Pregel: a system for large-scale graph processing,” in *Proceedings of the 2010 ACM SIGMOD International Conference on Management of Data*, ser. SIGMOD ’10. New York, NY, USA: Association for Computing Machinery, 2010, p. 135–146. [Online]. Available: <https://doi.org/10.1145/1807167.1807184>
- [32] D. Yan, J. Cheng, Y. Lu, and W. Ng, “Effective techniques for message reduction and load balancing in distributed graph computation,” in *Proceedings of the 24th International Conference on World Wide Web*, 2015, pp. 1307–1317.
- [33] Y. Low, J. Gonzalez, A. Kyrola, D. Bickson, C. Guestrin, and J. M. Hellerstein, “Distributed graphlab: A framework for machine learning in the cloud,” *arXiv preprint arXiv:1204.6078*, 2012.
- [34] J. E. Gonzalez, Y. Low, H. Gu, D. Bickson, and C. Guestrin, “PowerGraph: Distributed Graph-Parallel computation on natural graphs,” in *10th USENIX Symposium on Operating Systems Design and Implementation (OSDI)*, 2012, pp. 17–30.
- [35] M. Han and K. Daudjee, “Giraph unchained: Barrierless asynchronous parallel execution in pregel-like graph processing systems,” *Proceedings of the VLDB Endowment*, vol. 8, no. 9, pp. 950–961, 2015.
- [36] S. Salihoglu and J. Widom, “Gps: A graph processing system,” in *Proceedings of the 25th International Conference on Scientific and Statistical Database Management*, 2013, pp. 1–12.
- [37] A. Roy, I. Mihailoel, and W. Zwaenepoel, “X-stream: Edge-centric graph processing using streaming partitions,” in *Proceedings of the Twenty-Fourth ACM Symposium on Operating Systems Principles*, 2013, pp. 472–488.
- [38] H. Zhu, L. He, M. Leeke, and R. Mao, “Wolfgraph: The edge-centric graph processing on gpu,” *Future Generation Computer Systems*, vol. 111, pp. 552–569, 2020.
- [39] Y. Tian, A. Balmin, S. A. Corsten, S. Tatikonda, and J. McPherson, “From “think like a vertex” to “think like a graph”,” *Proceedings of the VLDB Endowment*, vol. 7, no. 3, pp. 193–204, 2013.
- [40] Y. Simmhan, A. Kumbhare, C. Wickramaarachchi, S. Nagarkar, S. Ravi, C. Raghavendra, and V. Prasanna, “Goffish: A sub-graph centric framework for large-scale graph analytics,” in *European Conference on Parallel Processing*. Springer, 2014, pp. 451–462.
- [41] D. Yan, J. Cheng, Y. Lu, and W. Ng, “Blugel: A block-centric framework for distributed computation on real-world graphs,” *Proceedings of the VLDB Endowment*, vol. 7, no. 14, pp. 1981–1992, 2014.
- [42] F. Harary, “On the notion of balance of a signed graph,” *Michigan Mathematical Journal*, vol. 2, no. 2, pp. 143–146, 1953.
- [43] T. Zaslavsky, “A mathematical bibliography of signed and gain graphs and allied areas,” *The Electronic Journal of Combinatorics*, pp. DS8–Dec, 2012.
- [44] D. Cartwright and F. Harary, “Structural balance: a generalization of heider’s theory,” *Psychological Review*, vol. 63, no. 5, pp. 277–293, 1956.
- [45] M. Brusco and D. Steinley, “Relational and signed network clustering via relaxations of the frustration index,” *Journal of Mathematical Psychology*, vol. 90, pp. 16–29, 2019.
- [46] J. C. Boschero, N. M. Neumann, W. van der Schoot, T. Sijpesteijn, and R. Wezeman, “Distributed quantum computing: Applications and challenges,” in *Intelligent Computing-Proceedings of the Computing Conference*. Springer, 2025, pp. 100–116.
- [47] A. Shukla and P. Vedula, “An efficient quantum algorithm for preparation of uniform quantum superposition states,” *Quantum Information Processing*, vol. 23, no. 2, Jan. 2024.
- [48] G. Lüders, “Über die zustandsänderung durch den meßprozeß,” *Annalen der Physik*, vol. 443, no. 5–8, pp. 322–328, 1950.

## A Classical Simulation of Quantum Sketch

Here we provide the Python code that implements the quantum sketch functionality.

```

1 from random import random
2 class QuantumSketch:
3     def __init__(self, items: set):
4         self.items = items
5         self.underlying = []
6
7     def query_pair(self, x, y):

```

```

8         if (x in self.items) and (y in self.items):
9             if random() < 2.0 / len(self.items):
10                self.items = []
11                return +1
12            else:
13                self.items.remove(x)
14                self.items.remove(y)
15                return 0
16
17        elif (x in self.items) or (y in self.items):
18            if random() < 1.0 / len(self.items):
19                self.items = []
20                if random() < 0.5:
21                    return -1
22                else:
23                    return +1
24            else:
25                self.items.discard(x)
26                self.items.discard(y)
27                return 0
28
29        else:
30            return 0
31
32    def update(self, x, l):
33        self.items.remove(l)
34        self.items.add(x)

```

Listing 1. Python implementation of the classical simulation of the quantum Sketch functionality.

## B Random Signed Graph Parameters Calculations

Here we describe in more detail the graphs generated for the numerical experiments. We generate random Erdős–Rényi with  $p_e$  the probability that an edge exists and  $p_+$  the probability that a given edge has sign +1. These theoretical values can then be used when implementing and running the  $T_1$  estimators, since these values are used in the number of resources required to run the algorithms themselves. For real-world graphs, these values can be estimated base on historical data.

### B.1 $|T_1|$ Expectation and Variance Calculations

**Lemma 9.**

$$\mathbb{E}[|T_1|] = 3 \binom{n}{3} p_e^3 p_+ (1 - p_+)^2, \quad (10)$$

$$\text{Var}(|T_1|) = 3 \binom{n}{3} p_e^3 p_+ (1 - p_+)^2 (1 - 3p_e^3 p_+ (1 - p_+)^2) \quad (11)$$

$$+ 2 \binom{n}{2} \binom{n-2}{2} (p_e^5 p_+ (1 - p_+)^3 (1 + 3p_+) - 9p_e^6 p_+ (1 - p_+)^4) \quad (12)$$

**PROOF.** Consider three distinct vertices  $u, v, w \in V$ . The probability they form a triangle is  $p_e^3$ . Let  $I_{uvw}$  be the indicator variable that is 1 if  $uvw$  is a  $T_1$ . The probability that the edges are a single  $-1$  and two  $+1$ s is  $p_+(1 - p_+)^2$ . There are three such ways for this to occur. So,  $\mathbb{P}[I_{uvw} = 1] = 3p_+(1 - p_+)^2$ . Noting that there are  $\binom{n}{3}$  such triples, we get

$$\mathbb{E}[|T_1|] = 3 \binom{n}{3} p_e^3 p_+(1-p_+)^2 \quad (13)$$

Onto the variance. Let  $p_\tau := \mathbb{P}[I_\tau]$  for a triple  $\tau$ . The variance can be calculated as

$$\text{Var}(|T_1|) = \sum_{\tau} \text{Var}(I_\tau) + 2 \sum_{\tau < \tau'} \text{Cov}(I_\tau, I_{\tau'}) \quad (14)$$

Since  $I_\tau$  is Bernoulli, we have  $\text{Var}(I_\tau) = p_\tau(1-p_\tau^2)$ . For the covariance, let  $uvw$  and  $xyz$  be two triangles. We need to understand what happens when they share vertices.

- When  $\{u, v, w\} \cap \{x, y, z\} = \emptyset$ , these triangles are independent and the covariance is 0.
- When  $|\{u, v, w\} \cap \{x, y, z\}| = 1$ , these triangles are independent and the covariance is 0.
- Assume  $|\{u, v, w\} \cap \{x, y, z\}| = 2$ . Without loss of generality, they share edge  $(u, v)$  and  $w \neq z$ . If  $\sigma_{uv} = -1$ , then the remaining 4 edges all must have  $+1$  sign, which occurs with probability  $p_+^4$ . On the other hand, if  $\sigma_{uv} = +1$ , then 1 of  $\sigma_{uw}, \sigma_{vw}$  must be  $+1$  and one must be  $-1$ , and the same for  $\sigma_{uz}, \sigma_{vz}$ . Each occurs with probability  $p_+^2(1-p_+)^2$ . Putting these together, we get

$$p_+(1-p_+)^4 + 4p_+^2(1-p_+)^3 = p_+(1-p_+)^3(1+3p_+). \quad (15)$$

- When  $|\{u, v, w\} \cap \{x, y, z\}| = 3$ , these triangles are the same and the covariance is 0.

The only non-zero case is when they share a single edge which allows us to calculate

$$\mathbb{P}[I_\tau, I_{\tau'} = 1] = p_e^5 p_+(1-p_+)^3(1+3p_+) \quad (16)$$

$$\Rightarrow \text{Cov}(I_\tau, I_{\tau'}) = p_e^5 p_+(1-p_+)^3(1+3p_+) - p_\tau^2 \quad (17)$$

$$= p_e^5 p_+(1-p_+)^3(1+3p_+) - 9p_e^6 p_+^2(1-p_+)^4. \quad (18)$$

Note that there are  $\binom{n}{2} \binom{n-2}{2}$  ways that the pair of triangles share an edge. We can now calculate the full variance:

$$\text{Var}(|T_1|) = \binom{n}{3} p_{uvw}(1-p_{uvw}) + 2 \binom{n}{2} \binom{n-2}{2} [p_e^5 p_+(1-p_+)^3(1+3p_+) - p_{uvw}^2] \quad (19)$$

$$\begin{aligned} &= 3 \binom{n}{3} p_e^3 p_+(1-p_+)^2(1-3p_e^3 p_+(1-p_+)^2) \\ &\quad + 2 \binom{n}{2} \binom{n-2}{2} (p_e^5 p_+(1-p_+)^3(1+3p_+) - 9p_e^6 p_+^2(1-p_+)^4) \end{aligned} \quad (20)$$

□

## B.2 $\Delta_{E_1}$ Expectation Calculation

Next we are interested in understanding  $\Delta_{E_1}$ , the maximum number of  $T_1$  triangles that share an edge. Let  $Y_e$  be the number of  $T_1$ s that share edge  $e$ . Then  $\Delta_{E_1} = \max_e Y_e$ . Therefore, we study  $\Delta_{E_1}$  via  $Y_e$ .

Fix edge  $e = (u, v)$ . We can further define the indicator  $Y_{uvw}$  to be 1 when  $uvw$  forms a  $T_1$ . The probability that  $uw$  and  $vw$  are both edges is  $p_e^2$ . If  $\sigma_{uv} = +1$ , then both of the other signs must be  $-1$ , which occurs with probability  $(1-p_+)^2$ . Otherwise, one of the edges is  $+1$  and  $-1$ . These individually occur with probability  $p_+(1-p_+)$  and there are 2 ways for this to occur. Therefore:

$$\mathbb{P}[Y_{uvw} = 1] = p_e^2 \left[ \overbrace{p_+}^{\sigma_{uv}=+1} (1-p_+)^2 + \overbrace{(1-p_+)}^{\sigma_{uv}=-1} \cdot 2p_+(1-p_+) \right] \quad (21)$$

$$= 3p_e^2 p_+(1-p_+)^2 \quad (22)$$

Let  $q_{uvw} := \mathbb{P}[Y_{uvw} = 1]$ . Since edges and their signs are independent,  $Y_{uv} \sim \text{Bin}(n-2, q_{uvw})$  which gives

$$\mathbb{E}[Y_{uv}] = (n-2)q_{uvw}, \quad \text{Var}(Y_{uv}) = (n-2)q_{uvw}(1-q_{uvw}). \quad (23)$$

Next, let  $M$  be the random variable for the number of edges in the graph. This is another Binomial variable of size  $\binom{n}{2}$  with success probability  $p_e$ . In particular,  $\mathbb{E}[M] \approx \frac{n^2}{2}p_e$ .

Binomials are sub-Gaussian, satisfying

$$\mathbb{P}\left[Y_e - \mathbb{E}[Y_e] > t\right] \leq \exp\left(-t^2/2 \text{Var}(Y_e)\right) \quad (24)$$

Therefore via a simple union bound:

$$\mathbb{P}\left[\max_{i=1, \dots, M} Y_i \geq \mathbb{E}[Y_i] + t\right] = \mathbb{P}\left[\bigcup_i \{Y_i - \mathbb{E}[Y_i] \geq t\}\right] \leq \sum_i \mathbb{P}\left[Y_e - \mathbb{E}[Y_e] > t\right] \quad (25)$$

$$\leq M \exp\left(-t^2/2 \text{Var}(Y_e)\right). \quad (26)$$

Letting  $t = \sqrt{2 \text{Var}(Y_e) \log M}$  leads to the statement

$$\mathbb{E}[\Delta_{E_1}] \lesssim (n-2)q_{uvw} + \sqrt{2(n-2)q_{uvw}(1-q_{uvw}) \log(n^2 p_e)}. \quad (27)$$

## C Quantum Streaming Primitives

In this section, we outline the quantum streaming paradigm used in Alg. 3. For convenience, we have renamed some methods used in Ref. [1]; see their manuscript for a more general treatment of this paradigm.

### C.1 Quantum Registers

Let  $n$  and  $m$  be the number of vertices and edges in our graph. Our *symbolic* universe for the sketch will be  $U = \{(u, v) \times \{+, -\} : u, v \in [n]\} \cup \{(\ell, \xi) : \ell \in [2m]\}$ , where  $\xi$  denotes a scratch symbol. To be concrete and illustrative of the underlying logic, we consider a case where  $n$  is a power of 2. Then the wavefunction state is decomposable as:

$$|Q\rangle = \sum_{j=0}^{n-1} \sum_{k=0}^{n-1} \sum_{s=0}^1 \sum_{t=0}^1 \alpha_{jkst} \underbrace{|j\rangle_{\log(n)} \otimes |k\rangle_{\log(n)}}_{\text{index register}} \otimes \underbrace{|s\rangle_1}_{\text{sign register}} \otimes \underbrace{|t\rangle_1}_{\text{scratch register}}, \quad (28)$$

where a state  $|j\rangle_{\log(n)}$  is the bit-wise decomposition  $j \in [n]$  over  $\log(n)$  qubits in the computational basis with state normalization  $\sum_{jkst} \overline{\alpha_{jkst}} \alpha_{jkst} = 1$ .

We show how each element from our *symbolic* universe maps to a concrete basis element of our quantum wavefunction. We define a scratch state as

$$|\ell, \xi\rangle \equiv |q\rangle_{\log(n)} |r\rangle_{\log(n)} |0\rangle_1 |0\rangle_1, \quad (29)$$

where  $\ell = qn + r$  such that the quotient  $q \in [n]$  and the remainder  $r \in [n]$ .

We define an edge state as:

$$|u, v, \sigma_{uv}\rangle \equiv |u\rangle_{\log(n)} |v\rangle_{\log(n)} |\sigma_{uv}\rangle_1 |1\rangle_1 \quad (30)$$

Given noiseless application of all quantum operation as described in Figure 3, assuming the algorithm has not exited yet, the state of the system can be described at the end of any timestamp  $\ell$  by the following lemma.

**Lemma 10** (Sketchpad State After  $\ell$  Edges). *For all  $\ell = 0, \dots, m-1$ , after the algorithm has processed  $\ell$  edges, if it has not yet terminated the underlying set of  $\mathcal{Q}_{S_\ell}$  is*

$$\mathcal{S}_\ell := \{(j, \xi) : j = 2\ell, \dots, 2m-1\} \cup \mathcal{K}_\ell \quad (31)$$

where

$$\mathcal{K}_\ell := \left\{ (u, v, \sigma_{uv}) : \left( \exists i \in [\ell] \text{ s.t. } (u, v, \sigma_{uv}) = (e_i, \sigma_i) \right) \wedge \left( \forall_{j=i+1, \dots, \ell} (g(j) = 0) \vee (v \notin e_j) \vee ((\sigma_j = +) \wedge (\sigma_{uv} = +)) \right) \right\} \quad (32)$$

where  $(e_i, \sigma_i)$  denotes the  $i^{\text{th}}$  signed edge in the stream. The size of  $\mathcal{S}_\ell$  is  $|\mathcal{S}_\ell| = 2m - 2\ell + |\mathcal{K}_\ell|$ .

In particular, after processing  $\ell$  edges from the stream, if the algorithm has not returned, the quantum state of the sketch is

$$|\mathcal{Q}_{S_\ell}\rangle = \frac{1}{\sqrt{2m - 2\ell + |\mathcal{K}_\ell|}} \left( \sum_{j=2\ell}^{2m-1} |j, \xi\rangle + \sum_{(u, v, \sigma_{uv}) \in \mathcal{K}_\ell} |u, v, \sigma_{uv}\rangle \right) \quad (33)$$

The set  $\mathcal{K}_\ell$  contains all edges that we have seen that have not been deleted. Assume  $(uv, \sigma_{uv})$  is an edge processed sometime before the  $\ell^{\text{th}}$  update. Consider timestep  $j = i + 1, \dots, \ell$ . Then  $(uv, \sigma_{uv})$  remains in the sketch iff:

- (1)  $g(j) = 0$  and thus no measurements are made at all.
- (2)  $v$  does not participate in the  $j^{\text{th}}$  edge and thus has no chance of being deleted.
- (3)  $v$  is in the  $j^{\text{th}}$  edge but both  $\sigma_{uv}, \sigma_j = +1$ . This is due to the fact that the  $j^{\text{th}}$  set of measurements resulted in a  $\perp$  but since  $\sigma_j = +1$ , we did not delete  $+1$ -neighbors.

See Section D.1 for a formal proof of this lemma.

## C.2 Measurement Operators

Here we describe the projective value measurements (PVMs) used to implement the `query_edges` calls used by Alg. 3. Recall that the quantum sketch is a superposition of at most  $2m$  computational basis states. The states with non-zero amplitude can be described in two different ways. The first are states  $|t, 0, 0\rangle$  where  $t \in [2m]$  and the 3rd register denotes this is a “scratch” state. Secondly, we have states like  $|v, w, \pm, 1\rangle$  where the first two registers  $v, w \in V$  are vertices, the third register is  $vw$ ’s sign  $\sigma_{vw}$ , and the fourth register denotes “active” status. This allows us to query for active states without worrying about conflicts of  $t = (v, w)$  (as bitstrings).

Consider the scenario in which we are processing edge  $vw$  with sign  $+1$ , leading to **step 8**. We want to query our sketch for a wedge  $uv, uw$  such that both of the edges have  $-1$  sign, thus completing a  $T_1$  triangle with  $uv$ . This is accomplished by the `query_edges((u, v, -), (u, w, -))` call

in **step 8** of Alg. 3. The following three operators form the PVM of this operation  $\mathcal{M}_{uv-,uw-} := \{O_{uv-,uw-}^{+1}, O_{uv-,uw-}^{-1}, O_{uv-,uw-}^{\perp}\}$ :

$$O_{uv-,uw-}^{+1} := \frac{1}{2} \left( |u, v, -\rangle + |u, w, -\rangle \right) \left( \langle u, v, -| + \langle u, w, -| \right), \quad (34)$$

$$O_{uv-,uw-}^{-1} := \frac{1}{2} \left( |u, v, -\rangle - |u, w, -\rangle \right) \left( \langle u, v, -| - \langle u, w, -| \right), \quad (35)$$

$$O_{uv-,uw-}^{\perp} := I - O_{uv-,uw-}^{+1} - O_{uv-,uw-}^{-1}. \quad (36)$$

The observables  $O_{uv-,uw-}^{+1}, O_{uv-,uw-}^{-1}$  are rank-1 projection operators onto two Bell-like states  $\frac{1}{\sqrt{2}} (|u, v, -\rangle \pm |u, w, -\rangle)$ .

Consider the scenario in which we are processing edge  $vw$  with sign  $-1$ , leading to **steps 11-13**. We want to query our sketch for a wedge  $uv, uw$  such that one of the edges has a  $+1$  sign and the other  $-1$ , thus completing a  $T_1$  triangle. This is accomplished by the `query_edges((u, v, +), (u, w, -))` call in **step 11** of Alg. 3. The following three operators form the PVM of this operation  $\mathcal{M}_{uv+,uw-} := \{O_{uv+,uw-}^{+1}, O_{uv+,uw-}^{-1}, O_{uv+,uw-}^{\perp}\}$ :

$$O_{uv+,uw-}^{+1} := \frac{1}{2} \left( |u, v, +\rangle + |u, w, -\rangle \right) \left( \langle u, v, +| + \langle u, w, -| \right), \quad (37)$$

$$O_{uv+,uw-}^{-1} := \frac{1}{2} \left( |u, v, +\rangle - |u, w, -\rangle \right) \left( \langle u, v, +| - \langle u, w, -| \right), \quad (38)$$

$$O_{uv+,uw-}^{\perp} := I - O_{uv+,uw-}^{+1} - O_{uv+,uw-}^{-1}. \quad (39)$$

The superscript in  $O_{uv+,uw-}^{\pm 1}$  refers to this being a projection onto the superposition state  $\frac{1}{\sqrt{2}} (|u, v, +\rangle \pm |u, w, -\rangle)$ . The fourth register being set to 1 is used to only query for “active” data states and in particular, *not* query for scratch states. The PVM on **step 13** of Alg. 3 follows similarly,  $\mathcal{M}_{uv-,uw+} := \{O_{uv-,uw+}^{+1}, O_{uv-,uw+}^{-1}, O_{uv-,uw+}^{\perp}\}$ :

$$O_{uv-,uw+}^{+1} := \frac{1}{2} \left( |u, v, -\rangle + |u, w, +\rangle \right) \left( \langle u, v, -| + \langle u, w, +| \right), \quad (40)$$

$$O_{uv-,uw+}^{-1} := \frac{1}{2} \left( |u, v, -\rangle - |u, w, +\rangle \right) \left( \langle u, v, -| - \langle u, w, +| \right), \quad (41)$$

$$O_{uv-,uw+}^{\perp} := I - O_{uv-,uw+}^{+1} - O_{uv-,uw+}^{-1}. \quad (42)$$

Similarly to the PVMs of step 8,  $O_{uv-,uw+}^{\pm 1}$  are projections onto the superposition state  $\frac{1}{\sqrt{2}} (|u, v, -\rangle \pm |u, w, +\rangle)$  respectively.

### C.3 Circuit Primitives

We now explain the three quantum sub-circuits necessary for Alg. 3: `create`, `insert`, and `query_edges`.

The 3 quantum operations are detailed as follows.

**C.3.1 create.** This method instantiates the sketch by creating a superposition of  $2m$  computational basis states. Here,  $\mathcal{S}_0 := \{(j, \xi) : j = 0, \dots, 2m - 1\}$  and we have

$$|Q_{\mathcal{S}_0}\rangle = \frac{1}{\sqrt{2m}} \sum_{j=0}^{2m-1} |j, \xi\rangle \quad (43)$$

When  $m$  is a power of 2, this can be done simply with Hadamard; if not, this can still be done efficiently [47].

C.3.2 `insert((vw,  $\sigma_{vw}$ ),  $\ell$ ,  $Q_S$ )`. Stores  $(vw, \sigma_{vw})$  into the sketch  $\mathcal{S}$ . This operation “uses” two scratch states by rotating them to  $|v, w, \sigma_{vw}\rangle$  and  $|w, v, \sigma_{vw}\rangle$ .

Suppose we are in step  $\ell$ . We perform permutation  $\pi_{\ell, vw, \sigma_{vw}}$  that swaps:

- $(2\ell, \xi)$  for  $(v, w, \sigma_{vw})$
- $(2\ell + 1, \xi)$  for  $(w, v, \sigma_{vw})$

Since we process an edge on pair  $\{v, w\}$  only once, this swap has the effect of mapping the state  $|2\ell, \xi\rangle$  to a state  $|v, w, \sigma_{vw}\rangle$  and the state  $|2\ell + 1, \xi\rangle$  to a state  $|w, v, \sigma_{vw}\rangle$  which is equivalent to the mappings

$$|v, w, \sigma_{vw}\rangle\langle 2\ell, \xi| \equiv |v\rangle\langle q_{2\ell}| \otimes |w\rangle\langle r_{2\ell}| \otimes |\sigma_{vw}\rangle\langle 0| \otimes |1\rangle\langle 0|, \quad (44)$$

$$|w, v, \sigma_{vw}\rangle\langle 2\ell + 1, \xi| \equiv |w\rangle\langle q_{2\ell+1}| \otimes |v\rangle\langle r_{2\ell+1}| \otimes |\sigma_{vw}\rangle\langle 0| \otimes |1\rangle\langle 0|, \quad (45)$$

where  $2\ell = q_{2\ell} n + r_{2\ell}$  and  $2\ell + 1 = q_{2\ell+1} n + r_{2\ell+1}$ .

The entire unitary at this point (so as not to disturb the rest of the state) is simply identity on all other states:

$$U_{\pi_{\ell, vw, \sigma_{vw}}} = \begin{aligned} & I - |2\ell, \xi\rangle\langle 2\ell, \xi| - |v, w, \sigma_{vw}\rangle\langle v, w, \sigma_{vw}| \\ & + |v, w, \sigma_{vw}\rangle\langle 2\ell, \xi| + |2\ell, \xi\rangle\langle v, w, \sigma_{vw}| \\ & - |2\ell + 1, \xi\rangle\langle 2\ell + 1, \xi| - |w, v, \sigma_{vw}\rangle\langle w, v, \sigma_{vw}| \\ & + |v, w, \sigma_{vw}\rangle\langle 2\ell + 1, \xi| + |2\ell + 1, \xi\rangle\langle v, w, \sigma_{vw}| \end{aligned} \quad (46)$$

C.3.3 `query_edges`. The operation `query_edges((wu,  $\tau_{wu}$ ), (wv,  $\tau_{wv}$ ))` queries  $\mathcal{S}$  for a wedge  $(wu, wv)$  that would complete a triangle with  $uv$  (along with edge information). This is done by making a measurement on  $Q_S$ . There are three possible scenarios: (I) both signed edges are in the current sketch, (II) only one of them is in the sketch, and (III) neither of them is in the sketch. Depending on which scenario is currently applicable, the following describes the possible outcomes with their associated probabilities.

- (I) (a) With probability  $2/|\mathcal{S}|$ , destroy  $Q_S$  and return +1.  
(b) With probability  $1 - 2/|\mathcal{S}|$ , the sketch is updated to  $\mathcal{S}' = \mathcal{S} \setminus \{(wu, \tau_{wu}), (wv, \tau_{wv})\}$  and  $Q_S$  is updated to  $Q_{\mathcal{S}'}$ . Return  $\perp$ .
- (II) (a) With probability  $1/|\mathcal{S}|$ , destroy  $Q_S$  and with equal probability return  $\{+1, -1\}$ .  
(b) With probability  $1 - 1/|\mathcal{S}|$ , the sketch is updated to  $\mathcal{S}' = \mathcal{S} \setminus \{(wu, \tau_{wu}), (wv, \tau_{wv})\}$  and  $Q_S$  is updated to  $Q_{\mathcal{S}'}$ . Return  $\perp$ .
- (III) Leave  $Q_S$  unchanged and return  $\perp$ .

This query method is done by making measurements onto the quantum state  $|Q_S\rangle$  as outlined in Section C.2. We work through the steps here for the measurement collection  $\mathcal{M}_{wu-, wv+} = \{O_{wu-, wv+}^{+1}, O_{wu-, wv+}^{-1}, O_{wu-, wv+}^{\perp}\}$  although similar logic can be used for  $\mathcal{M}_{wu-, wv-}$ ,  $\mathcal{M}_{wu+, wv-}$ .

At the point of measurement, the wavefunction of the system is

$$|Q_S\rangle = \frac{1}{\sqrt{|\mathcal{S}|}} \left( \sum_{j=2\ell}^{2m-1} |j, \xi\rangle + \sum_{(u, v, \sigma_{uv}) \in \mathcal{S}} |u, v, \sigma_{uv}\rangle \right) \quad (47)$$

- (I) (a) With probability  $2/|\mathcal{S}|$ , destroy  $Q_S$  and return +1.  
(b) With probability  $1 - 2/|\mathcal{S}|$ , the sketch is updated to  $\mathcal{S}' = \mathcal{S} \setminus \{(wu, \tau_{wu}), (wv, \tau_{wv})\}$  and  $Q_S$  is updated to  $Q_{\mathcal{S}'}$ . Return  $\perp$ .

In scenario I,  $(w, u, -), (w, v, +) \in \mathcal{S}$ . Then

$$\langle Q_S | O_{wu-,wv+}^{+1} | Q_S \rangle = \langle Q_S | \frac{1}{2} (|w, u, -\rangle + |w, v, +\rangle) ( \langle w, u, -| + \langle w, v, +| ) | Q_S \rangle \quad (48)$$

$$= \frac{1}{2} \left( \frac{1}{\sqrt{|\mathcal{S}|}} + \frac{1}{\sqrt{|\mathcal{S}|}} \right) \left( \frac{1}{\sqrt{|\mathcal{S}|}} + \frac{1}{\sqrt{|\mathcal{S}|}} \right) \quad (49)$$

$$= \frac{2}{|\mathcal{S}|}, \quad (50)$$

and

$$\langle Q_S | O_{wu-,wv+}^{-1} | Q_S \rangle = \langle Q_S | \frac{1}{2} (|w, u, -\rangle - |w, v, +\rangle) ( \langle w, u, -| - \langle w, v, +| ) | Q_S \rangle \quad (51)$$

$$= \frac{1}{2} \left( \frac{1}{\sqrt{|\mathcal{S}|}} - \frac{1}{\sqrt{|\mathcal{S}|}} \right) \left( \frac{1}{\sqrt{|\mathcal{S}|}} - \frac{1}{\sqrt{|\mathcal{S}|}} \right) \quad (52)$$

$$= 0, \quad (53)$$

and

$$\langle Q_S | O_{wu-,wv+}^\perp | Q_S \rangle = \langle Q_S | I - O_{wu-,wv+}^{+1} - O_{wu-,wv+}^{-1} | Q_S \rangle \quad (54)$$

$$= 1 - \frac{2}{|\mathcal{S}|}. \quad (55)$$

In the case that  $O_{wu-,wv+}^+$  was observed, the wavefunction collapsed into the 1-dimensional space unambiguously. In the case  $O_{wu-,wv+}^\perp$  was observed, the wavefunction is given by Lüder's post-measurement update rule [48]:

$$\frac{O_{wu-,wv+}^\perp | Q_S \rangle}{\|O_{wu-,wv+}^\perp | Q_S \rangle\|} = \frac{1}{\|O_{wu-,wv+}^\perp | Q_S \rangle\|} \frac{1}{\sqrt{|\mathcal{S}|}} \left( \sum_{j=2\ell}^{2m-1} |j, \xi\rangle + \sum_{(u,v,\sigma_{uv}) \in \mathcal{S} \setminus \{(w,u,-), (w,v,+)\}} |u, v, \sigma_{uv}\rangle \right) \quad (56)$$

$$= \frac{\sqrt{|\mathcal{S}|}}{\sqrt{|\mathcal{S}|} - 2} \frac{1}{\sqrt{|\mathcal{S}|}} \left( \sum_{j=2\ell}^{2m-1} |j, \xi\rangle + \sum_{(u,v,\sigma_{uv}) \in \mathcal{S} \setminus \{(w,u,-), (w,v,+)\}} |u, v, \sigma_{uv}\rangle \right) \quad (57)$$

$$= \frac{1}{\sqrt{|\mathcal{S}|} - 2} \left( \sum_{j=2\ell}^{2m-1} |j, \xi\rangle + \sum_{(u,v,\sigma_{uv}) \in \mathcal{S} \setminus \{(w,u,-), (w,v,+)\}} |u, v, \sigma_{uv}\rangle \right) \quad (58)$$

- (II) (a) With probability  $1/|\mathcal{S}|$ , destroy  $Q_S$  and with equal probability return  $\{+1, -1\}$ .  
 (b) With probability  $1 - 1/|\mathcal{S}|$ , the sketch is updated to  $\mathcal{S}' = \mathcal{S} \setminus \{(wu, \tau_{wu}), (wv, \tau_{wv})\}$  and  $Q_S$  is updated to  $Q_{\mathcal{S}'}$ . Return  $\perp$ .

In scenario II, only one of  $(w, u, -), (w, v, +)$  is in  $\mathcal{S}$ . Then

$$\langle Q_S | O_{wu-,wv+}^{+1} | Q_S \rangle = \langle Q_S | \frac{1}{2} (|w, u, -\rangle + |w, v, +\rangle) ( \langle w, u, -| + \langle w, v, +| ) | Q_S \rangle \quad (59)$$

$$= \frac{1}{2} \left( \frac{1}{\sqrt{|\mathcal{S}|}} \right) \left( \frac{1}{\sqrt{|\mathcal{S}|}} \right) \quad (60)$$

$$= \frac{1}{2|\mathcal{S}|}, \quad (61)$$

and

$$\langle Q_S | O_{wu-,wv+}^{-1} | Q_S \rangle = \langle Q_S | \frac{1}{2} (|w, u, -\rangle - |w, v, +\rangle) (\langle w, u, -| - \langle w, v, +|) | Q_S \rangle \quad (62)$$

$$= \frac{1}{2} \left( \pm \frac{1}{\sqrt{|S|}} \right) \left( \pm \frac{1}{\sqrt{|S|}} \right) \quad (63)$$

$$= \frac{1}{2|S|}, \quad (64)$$

and

$$\langle Q_S | O_{wu-,wv+}^\perp | Q_S \rangle = \langle Q_S | I - O_{wu-,wv+}^{+1} - O_{wu-,wv+}^{-1} | Q_S \rangle \quad (65)$$

$$= 1 - \frac{1}{|S|}. \quad (66)$$

Similar to scenario *I*, if we observe  $O_{wu-,wv+}^{+1}, O_{wu-,wv+}^{-1}$ , the state has collapsed unambiguously into the 1-dimensional subspace. In the case  $O_{wu-,wv+}^\perp$  is observed, by the same logic as for scenario *I* we have that which ever element  $(w, u, -)$  or  $(w, v, +)$  present in  $S$  was deleted.

(III) Leave  $Q_S$  unchanged and return  $\perp$ . In this case it is clear that

$$\langle Q_S | O_{wu-,wv+}^{+1} | Q_S \rangle = 0 \quad (67)$$

$$\langle Q_S | O_{wu-,wv+}^{-1} | Q_S \rangle = 0 \quad (68)$$

and so

$$\langle Q_S | O_{wu-,wv+}^\perp | Q_S \rangle = \langle Q_S | I - O_{wu-,wv+}^{+1} - O_{wu-,wv+}^{-1} | Q_S \rangle \quad (69)$$

$$= 1. \quad (70)$$

Since neither were in the set, the wavefunction is also unchanged.

## D Analysis of Quantum Estimator

The main goal of this section is to prove Corollary 5. For clarity, we restate it here:

**Corollary 11.** *For any  $\varepsilon, \delta \in (0, 1]$ , there is a quantum streaming algorithm, using*

$$O \left( \frac{(km)^2 - (T_1^{<k})^2}{(T_1^{<k})^2} \log n \frac{1}{\varepsilon^2} \log \frac{1}{\delta} \right) \quad (71)$$

*quantum and classical bits, that estimates  $T_1^{<k}$  to  $\varepsilon T_1$  precision with probability  $1 - \delta$ .*

First, we need to show that the denominator matches (the square root of) the expectation of the algorithm:

**Lemma 12.**

$$\mathbb{E}[R_1^{<k}] = T_1^{<k} \quad (72)$$

Next, we will need that the numerator is the upper-bound on the variance:

**Lemma 13.**

$$\text{Var}(R_1^{<k}) \leq (km)^2 - (T_1^{<k})^2 \leq (km)^2 \quad (73)$$

Using these two facts, we are able to show that a median-of-means algorithm gives the desired performance and whose space matches that of Corollary 5. These statements will be proven later.

### D.1 Quantum Sketch Updates

In order to prove the desired statements above, we need to understand how the quantum sketch evolves as the algorithm progresses. For the rest of the section, let  $g : [m] \rightarrow \{0, 1\}$  be a fully independent hash function<sup>1</sup> such that

$$g(\ell) = \begin{cases} 1 & \text{with probability } 1/k \\ 0 & \text{otherwise.} \end{cases} \quad (74)$$

PROOF (LEMMA 10). We proceed by induction on  $\ell$ . For  $\ell = 0$ ,

$$\mathcal{S}_0 = \{(j, \xi) \mid j \in [2m]\} \quad (75)$$

since we prepared the uniform state

$$|Q_{\mathcal{S}_0}\rangle = \left( \frac{1}{\sqrt{2m}} \sum_{j=0}^{2m-1} |j\rangle_{2 \log(n)} \right) |0\rangle_1 |0\rangle_1 \quad (76)$$

$$= \frac{1}{\sqrt{2m}} \sum_{j=0}^{2m-1} |p_j\rangle_{\log(n)} |r_j\rangle_{\log(n)} |0\rangle_1 |0\rangle_1 \quad (77)$$

$$\equiv \frac{1}{\sqrt{2m}} \sum_{j=0}^{2m-1} |j, \xi\rangle \quad (\text{symbolic form, Eq. (29)}) \quad (78)$$

and so the result holds. We now prove by induction. For any  $\ell \in [m-1]$ , suppose that the result holds after  $\ell$  edges. Let  $(x, y, \sigma_{xy})$  (with  $x < y$ ) be the  $(\ell+1)$ <sup>th</sup> edge.

First consider the effect of the query\_edge operations. If  $g(\ell+1) = 0$ , they do not happen, and so  $\mathcal{S}$  and thus  $Q_{\mathcal{S}}$  are unchanged. If  $g(\ell+1) = 1$ , we can assume all of them return  $\perp$ , as otherwise the algorithm would terminate.

Suppose  $\sigma_{xy} = +$ , then on **step 8** we apply the query\_edges associated with  $(u, x, -)$ ,  $(u, y, -)$  for every  $u \in V$ . Then the associated state, in accordance with Section C.3.3, is:

$$|Q_{\mathcal{S}_{\ell+1}}\rangle = \frac{O_{ux-,uy-}^{\perp} |Q_{\mathcal{S}_{\ell}}\rangle}{\|O_{ux-,uy-}^{\perp} |Q_{\mathcal{S}_{\ell}}\rangle\|} \quad (79)$$

$$= \frac{1}{\|O_{ux-,uy-}^{\perp} |Q_{\mathcal{S}_{\ell}}\rangle\|} \left( I - O_{ux-,uy-}^{+1} - O_{ux-,uy-}^{-1} \right) |Q_{\mathcal{S}_{\ell}}\rangle \quad (80)$$

$$= \frac{1}{\|O_{ux-,uy-}^{\perp} |Q_{\mathcal{S}_{\ell}}\rangle\|} \left( |Q_{\mathcal{S}_{\ell}}\rangle - \left( \langle u, x, - | Q_{\mathcal{S}_{\ell}} \rangle \right) |u, x, -\rangle - \left( \langle u, y, - | Q_{\mathcal{S}_{\ell}} \rangle \right) |u, y, -\rangle \right) \quad (81)$$

In particular, the bracket inner products yield

$$\langle u, x, - | Q_{\mathcal{S}_{\ell}} \rangle = \begin{cases} \frac{1}{\sqrt{S_{\ell}}} & (u, x, -) \in \mathcal{K}_{\ell} \\ 0 & \text{otherwise} \end{cases}, \quad (82)$$

$$\langle u, y, - | Q_{\mathcal{S}_{\ell}} \rangle = \begin{cases} \frac{1}{\sqrt{S_{\ell}}} & (u, y, -) \in \mathcal{K}_{\ell} \\ 0 & \text{otherwise} \end{cases}. \quad (83)$$

<sup>1</sup>For each  $\ell \in [m]$  on step 5, we receive  $\log(n)$  random bits from our Random Number Generator.

So if  $(u, x, -)$  or  $(u, y, -)$  are in  $\mathcal{S}_\ell$ , they must have been deleted given that the measurement yielded  $\perp$ . Then after the loop of **step 6** finishes, we have deleted

$$\mathcal{D}_{\ell+1}^+ = \{(u, x, -) \in \mathcal{K}_\ell\} \cup \{(u, y, -) \in \mathcal{K}_\ell\} \quad (84)$$

$$= \{(u, z, -) \in \mathcal{K}_\ell : z \in \{x, y\}\} \quad (85)$$

and so

$$\mathcal{K}_{\ell+1} = \mathcal{K}_\ell \setminus \mathcal{D}_{\ell+1}^+ \cup \{(x, y, +)\} \cup \{(y, x, +)\}. \quad (86)$$

Then the underlying state after processing  $\ell + 1$  edges is

$$|Q_{\mathcal{S}_{\ell+1}}\rangle = \frac{1}{\sqrt{2m - 2\ell + |\mathcal{K}_\ell| - |\mathcal{D}_{\ell+1}^+|}} \left( \sum_{j=2\ell+2}^{2m-1} |j, \xi\rangle + |x, y, -\rangle + |y, x, -\rangle + \sum_{u,v,\sigma_{uv} \in \mathcal{K}_\ell \setminus \mathcal{D}_{\ell+1}^+} |u, v, \sigma_{uv}\rangle \right) \quad (87)$$

$$= \frac{1}{\sqrt{2m - 2\ell - 2 + |\mathcal{K}_{\ell+1}|}} \left( \sum_{j=2\ell+2}^{2m-1} |j, \xi\rangle + \sum_{u,v,\sigma_{uv} \in \mathcal{K}_{\ell+1}} |u, v, \sigma_{uv}\rangle \right) \quad (88)$$

Suppose  $\sigma_{xy} = -$ , then on **step 11** we apply `query_edges` associated with  $(u, x, +)$ ,  $(u, y, -)$  for every  $u \in V$ . Then the associated state is:

$$|Q_{\mathcal{S}_{\ell+1}}\rangle = \frac{O_{ux+,uy-}^\perp |Q_{\mathcal{S}_\ell}\rangle}{\|O_{ux+,uy-}^\perp |Q_{\mathcal{S}_\ell}\rangle\|} \quad (89)$$

$$= \frac{1}{\|O_{ux+,uy-}^\perp |Q_{\mathcal{S}_\ell}\rangle\|} \left( I - O_{ux+,uy-}^{+1} - O_{ux+,uy-}^{-1} \right) |Q_{\mathcal{S}_\ell}\rangle \quad (90)$$

$$= \frac{1}{\|O_{ux-,uy-}^\perp |Q_{\mathcal{S}_\ell}\rangle\|} \left( |Q_{\mathcal{S}_\ell}\rangle - \left( \langle u, x, + | Q_{\mathcal{S}_\ell} \rangle \right) |u, y, +\rangle - \left( \langle u, y, - | Q_{\mathcal{S}_\ell} \rangle \right) |u, y, -\rangle \right) \quad (91)$$

In particular, the bracket inner products yield

$$\langle u, x, + | Q_{\mathcal{S}_\ell} \rangle = \begin{cases} \frac{1}{\sqrt{S_\ell}} & (u, x, +) \in \mathcal{K}_\ell \\ 0 & \text{otherwise} \end{cases}, \quad (92)$$

$$\langle u, y, - | Q_{\mathcal{S}_\ell} \rangle = \begin{cases} \frac{1}{\sqrt{S_\ell}} & (u, y, -) \in \mathcal{K}_\ell \\ 0 & \text{otherwise} \end{cases}. \quad (93)$$

So if  $(u, x, +)$  or  $(u, y, -)$  are in  $\mathcal{S}_\ell$ , they must have been deleted given that the measurement yielded  $\perp$ . Then after the loop of **step 6** finishes, we have deleted

$$\mathcal{D}_{\ell+1}^{+-} = \{(u, x, +) \in \mathcal{K}_\ell\} \cup \{(u, y, -) \in \mathcal{K}_\ell\}, \quad (94)$$

Then on **step 13**, we similarly apply `query_edges` associated with  $(u, v, -)$ ,  $(u, y, +)$  for every  $u \in V$ . Then by a symmetric argument, the deleted set is

$$\mathcal{D}_{\ell+1}^{-+} = \{(u, x, -) \in \mathcal{K}_\ell\} \cup \{(u, y, +) \in \mathcal{K}_\ell\}, \quad (95)$$

The total deleted set after **steps 11-13** is then

$$\mathcal{D}_{\ell+1}^- = \mathcal{D}_{\ell+1}^{-+} \cup \mathcal{D}_{\ell+1}^{+-} \quad (96)$$

$$= \{(u, x, \sigma_{ux}) \in \mathcal{K}_\ell\} \cup \{(u, y, \sigma_{uy}) \in \mathcal{K}_\ell\} \quad (97)$$

$$= \{(u, z, \sigma_{uz}) \in \mathcal{K}_\ell : z \in \{x, y\}\} \quad (98)$$

And so the set after adding  $(x, y, -)$  and  $(y, x, -)$  is

$$\mathcal{K}_{\ell+1} = \mathcal{K}_{\ell} \setminus \mathcal{D}_{\ell+1}^- \cup \{(x, y, -)\} \cup \{(y, x, -)\} \quad (99)$$

Thus, their effect on the underlying set of  $\mathcal{Q}$  can be summarized over both scenarios if  $g(\ell+1) = 1$  as to delete

$$\mathcal{D}_{\ell+1} = \begin{cases} \{(u, z, -) \in \mathcal{K}_{\ell} : z \in \{x, y\}\} & \text{if } \sigma_{xy} = + \wedge g(\ell+1) = 1 \\ \{(u, z, \sigma_{uz}) \in \mathcal{K}_{\ell} : z \in \{x, y\}\} & \text{if } \sigma_{xy} = - \wedge g(\ell+1) = 1 \\ \emptyset & \text{otherwise.} \end{cases} \quad (100)$$

$$= \{(u, z, \sigma_{uz}) \in \mathcal{K}_{\ell} : z \in \{x, y\} \wedge (\sigma_{xy} = -1 \vee \sigma_{uz} = -1) \wedge (g(\ell+1) = 1)\} \quad (101)$$

from it. In words, negative or positive edges incident on  $xy$  are deleted if  $\sigma_{xy} = -$  while only negative edges incident on  $xy$  are deleted if  $\sigma_{xy} = +$ .

Then the updated set before and after calling insert is

$$\mathcal{K}_{\ell} \setminus \mathcal{D}_{\ell+1} = \{(u, v, \sigma_{uv}) \in \mathcal{K}_{\ell} : (g(\ell+1) = 0) \vee (v \notin xy) \vee (\sigma_{xy} = + \vee \sigma_{uv} = +)\}, \quad (102)$$

$$\mathcal{K}_{\ell+1} = \mathcal{K}_{\ell} \setminus \mathcal{D}_{\ell+1} \cup \{x, y, \sigma_{xy}\} \cup \{y, x, \sigma_{xy}\}, \quad (103)$$

which matches our expected lemma.

Specifically,  $\exists i \in [\ell+1]$  s.t.  $(u, v, \sigma_{uv}) = (e_i, \sigma_i)$  now includes  $(x, y, \sigma_{xy}), (y, x, \sigma_{xy})$  from  $i = \ell+1$  due to  $\text{insert}((xy, \sigma_{xy}), \mathcal{Q})$ . The condition:

$$\forall_{j=i+1, \dots, \ell+1} \left( g(j) = 0 \right) \vee \left( v \notin e_j \right) \vee \left( (\sigma_j = +) \wedge (\sigma_{uv} = +) \right) \quad (104)$$

reflects that  $\mathcal{D}_{\ell+1}$  is the empty set if  $g(\ell+1) = 0$ ; if not, then  $\mathcal{D}_{\ell+1}$  would include all negative or positive edges incident on  $(e_{\ell+1}, \sigma_{\ell+1})$  if  $\sigma_{\ell+1} = -$  or all negative incident edges if  $\sigma_{\ell+1} = +$ .  $\square$

In order to analyze the algorithm, we need to argue about the underlying sketch at different points in time. Let  $\mathcal{E}_T^{\ell}$  be the probability that the sketch was destroyed on step  $\ell$ . Let  $\mathcal{E}_{NT}^{\ell}$  be the event that the algorithm has not yet terminated by the end of processing the  $\ell^{\text{th}}$  edge. In particular, the quantum sketch still exists and has not collapsed and we have added the  $\ell^{\text{th}}$  edge to the sketch. Let  $\mathcal{E}_{\text{exit}}^{\ell}$  be the event that we exit the algorithm while processing the  $\ell^{\text{th}}$  edge.

**Lemma 14.** For any  $\ell \in [m]$ ,

$$\mathbb{P}[\mathcal{E}_{NT}^{\ell}] = \frac{|\mathcal{S}_{\ell}^{\ell}|}{2m}, \quad (105)$$

This can be seen as an application of Lemma 1 in Ref. [1].

**Lemma 15.** Let  $(vw, \sigma_{vw})$  be the  $\ell^{\text{th}}$  edge in a stream. Conditioned on  $\mathcal{E}_{NT}^{\ell-1}$ ,

- (a) If  $(uw, -) < (vw, \sigma_{vw})$ , then the probability that  $(uw, -)$  is still in the sketch is  $(1 - 1/k)^{d_{uw}}$ .
- (b) If  $(uw, +) < (vw, \sigma_{vw})$ , then the probability that  $(uw, +)$  is still in the sketch is  $(1 - 1/k)^{d_{uw}^-}$ .

In particular, a positive-signed edge can only be deleted by negative-signed neighbors.

**PROOF.** (a) By the definition of  $\mathcal{K}_{\ell-1}$ ,  $(uw, -)$  is in the sketch iff it entered at some time  $j < \ell$  and there were no signed edges incident to  $v$  that arrived after  $(uw, -)$  for an edge  $j < k < \ell$  such that  $g(k) = 1$ . Suppose  $vq$  is the  $k^{\text{th}}$  edge such that  $j < k < \ell$  and  $g(k) = 1$ . If  $\sigma_{vq} = -1$ , then the  $\text{query\_edges}((uq, +), (uv, -), \mathcal{Q})$  call in line 11 (conditioned on it returning  $\perp$ ) will delete  $(uv, -)$  from the sketch. Similarly,  $\sigma_{vq} = +1$ , then the  $\text{query\_edges}((uq, -), (uv, -), \mathcal{Q})$  call in line 8 deletes  $(uv, -)$  (conditioned on it returning  $\perp$ ). Either way, conditioned on reaching  $\ell$ , the only way for  $(uw, -)$  to still be in the sketch is for all incident edges to  $v$  to come after  $(uw, -)$  to not have

triggered the query operations. The  $j^{\text{th}}$  set of queries occur with probability  $1/k$ , so the probability that all the queries do **not** occur for every such  $j$  is given by  $(1 - 1/k)^{d_{uvw}^+ + d_{uvw}^-} = (1 - 1/k)^{d_{uvw}}$  since  $g$  is fully independent.

(b) By the definition of  $\mathcal{K}_{\ell-1}$ ,  $(uv, +)$  is in the sketch iff it entered at some time  $j < \ell$  and there were no **-1** signed edges incident to  $v$  that arrived after  $(uv, +)$  for an edge  $j < k < \ell$  such that  $g(k) = 1$ . Suppose  $vq$  is the  $k^{\text{th}}$  edge such that  $j < k < \ell$  and  $g(k) = 1$ . If  $\sigma_{vq} = -1$ , then the query\_edges( $(uq, -)$ ,  $(uv, +)$ ,  $\mathcal{Q}$ ) call in line 13 (conditioned on it returning  $\perp$ ) will delete  $(uv, -)$  from the sketch. On the other hand, if  $\sigma_{vq} = +1$ , then there is no way for  $(uv, +)$  to be deleted from the sketch. Even if  $g(k) = 1$ , the query\_edges( $(uq, -)$ ,  $(uv, -)$ ,  $\mathcal{Q}$ ) call in line 8 as no bearing on  $(uv, +)$ . Therefore, we just need to track the **-1** edges incident to  $v$  and thus the probability that  $(uv, +)$  is still in the sketch is  $(1 - 1/k)^{d_{uvw}^-}$ .  $\square$

## D.2 Signed Triangles in the Stream

Fix an ordering on the stream. For edges  $e, f$ , we use  $e < f$  to denote that  $e$  arrives before  $f$  in the stream. Fix vertices  $u, v, w \in V$  such that  $(uv, \sigma_{uv}) < (vw, \sigma_{vw})$ . Define the positive-degree  $d_{uvw}^+$  as the number of **+**-edges incident to  $v$  that arrive between  $(uv, \sigma_{uv})$  and  $(vw, \sigma_{vw})$  (not including these edges themselves). Similarly define  $d_{uvw}^-$ . The full degree is then  $d_{uvw} := d_{uvw}^+ + d_{uvw}^-$ .

$$t_{uvw,++}^{<k} = \begin{cases} (1 - 1/k)^{d_{uvw}^- + d_{uvw}^+} & \text{if } (uv, +) < (uw, -) < (vw, -) \text{ is a } T_1 \text{ in } G \\ 0 & \text{otherwise.} \end{cases} \quad (106)$$

$$t_{uvw,-+-}^{<k} = \begin{cases} (1 - 1/k)^{d_{uvw}^+ + d_{uvw}^-} & \text{if } (uv, -) < (uw, +) < (vw, -) \text{ is a } T_1 \text{ in } G \\ 0 & \text{otherwise.} \end{cases} \quad (107)$$

$$t_{uvw,--+}^{<k} = \begin{cases} (1 - 1/k)^{d_{uvw}^+ + d_{uvw}^-} & \text{if } (uv, -) < (uw, -) < (vw, +) \text{ is a } T_1 \text{ in } G \\ 0 & \text{otherwise.} \end{cases} \quad (108)$$

We write  $T_{+-}^{<k} := \sum_{(u,v,w) \in V^3} t_{uvw,+-}^{<k}$ . Similarly define  $T_{-+-}^{<k}$ ,  $T_{--+}^{<k}$  and let  $T_1^{<k} = T_{+-}^{<k} + T_{-+-}^{<k} + T_{--+}^{<k}$ .

Likewise, define

$$t_{uvw,++}^{>k} = \begin{cases} 1 - (1 - 1/k)^{d_{uvw}^- + d_{uvw}^+} & \text{if } (uv, +) < (uw, -) < (vw, -) \text{ is a } T_1 \text{ in } G \\ 0 & \text{otherwise.} \end{cases} \quad (109)$$

$$t_{uvw,-+-}^{>k} = \begin{cases} 1 - (1 - 1/k)^{d_{uvw}^+ + d_{uvw}^-} & \text{if } (uv, -) < (uw, +) < (vw, -) \text{ is a } T_1 \text{ in } G \\ 0 & \text{otherwise.} \end{cases} \quad (110)$$

$$t_{uvw,--+}^{>k} = \begin{cases} 1 - (1 - 1/k)^{d_{uvw}^+ + d_{uvw}^-} & \text{if } (uv, -) < (uw, -) < (vw, +) \text{ is a } T_1 \text{ in } G \\ 0 & \text{otherwise.} \end{cases} \quad (111)$$

and the corresponding  $T_{+-}^{>k}$ ,  $T_{-+-}^{>k}$ ,  $T_{--+}^{>k}$ ,  $T_1^{>k}$  values. Then  $T_1 = T_1^{<k} + T_1^{>k}$ .

Recall that  $R_1^{<k}$  is the output of Alg. 3. We break this random variable down further according to the different ways we can return from the algorithm. Consider the  $\ell^{\text{th}}$  edge  $(vw, \sigma_{vw})$ . We define the random variable  $R_{u,vw;\sigma_{uv}\sigma_{uw}\sigma_{vw}}$  for any  $u \in V$  and  $\sigma_{uv}, \sigma_{uw} \in \{\pm 1\}$  as follows. In any of the following cases,  $R_{u,vw;\sigma_{uv}\sigma_{uw}\sigma_{vw}} = 0$ :

- (1) If  $g(\ell) = 0$  which means we do not make any measurements (and thus cannot return on this edge), or
- (2) If any previous query\_edges operation destroys the sketch (and thus we do not even reach edge  $\ell$ ), or

- (3) The value  $r_{\sigma_{uv}\sigma_{uw}}$  returned by the measurement query\_edges( $(u, v, \sigma_{uv}), (u, w, \sigma_{uw})$ ) is equal to  $\perp$ .

Otherwise,  $R_{u,vw;\sigma_{uv}\sigma_{uw}\sigma_{vw}} = r_{\sigma_{uv}\sigma_{uw}} km$ . Define

$$R_{--+} = \sum_{(v < w) \in E} \sum_{u \in V} R_{u,vw;--+}, \quad (\text{from step 7}) \quad (112)$$

$$R_{+--} = \sum_{(v < w) \in E} \sum_{u \in V} R_{u,vw;+--}, \quad (\text{from step 10}) \quad (113)$$

$$R_{-+-} = \sum_{(v < w) \in E} \sum_{u \in V} R_{u,vw;-+-}. \quad (\text{from step 12}) \quad (114)$$

Then  $R_1^{<k} = R_{--+} + R_{-+-} + R_{+--}$ . The explicit ordering of the nodes in an edge in the summation is to avoid double-counting issues. E.g. consider the triangle  $(12, +) < (13, -) < (23, -)$ . The algorithm also ensures that, even if the edge is read as  $(32, -)$ , since  $2 < 3$ , the query\_edges( $(1, 2, +), (1, 3, -)$ ) call in line 10 is triggered. Therefore, we assume that  $v < w$  moving forward.

Before proving Lemma 12, we need to understand the individual  $\mathbb{E}[R_{u,vw;\sigma_{uv}\sigma_{uw}\sigma_{vw}}]$  values.

**Lemma 16.**

$$\mathbb{E}[R_{u,vw;--+}] = t_{uvw,--+}^{<k} + t_{u,wv,--+}^{<k} \quad (115)$$

Both values correspond to the triangle  $\{(uv, -), (uw, -), (vw, +)\}$  in which  $(vw, +)$  completes the triangle. Moreover, due to how these values are defined, one and only one can be non-zero but when it is, it is equal to  $(1 - 1/k)^{d_{uvw} + d_{u,wv}}$ . This will be helpful in the proof below.

PROOF. First, consider the case where  $t_{uvw,--+}^{<k} + t_{u,wv,--+}^{<k} = 0$ . By the definition of  $t_{uvw,--+}^{<k}$ , this implies that either  $\{(uv, -), (uw, -), (vw, +)\}$  is not a triangle in  $G$ , or that it is but at least one of  $(uv, -)$  or  $(uw, -)$  arrived after  $(vw, +)$  in the stream. In either case, by Lemma 10, at least one of  $(uv, -)$  and  $(uw, -)$  will not be in the sketch at the time the  $(vw, +)$  queries occur, if they occur at all. If neither edge is in the sketch, the query is guaranteed to return  $\perp$  and so  $\mathbb{E}[R_{u,vw;--+}] = 0$ . If exactly one of them is, then either the query returns  $\perp$  or it is equally likely to return 1 or  $-1$ , and so again  $\mathbb{E}[R_{u,vw;--+}] = 0$ . Either way,  $\mathbb{E}[R_{u,vw;--+}] = 0 = t_{uvw,--+}^{<k} + t_{u,wv,--+}^{<k}$ .

Now suppose  $t_{u,vw,--+}^{<k} + t_{u,wv,--+}^{<k} > 0$ . Note that at most, one of these terms can be non-zero. By definition,  $t_{u,vw,--+}^{<k} + t_{u,wv,--+}^{<k} = (1 - 1/k)^{d_{uvw} + d_{u,wv}}$  no matter which term is non-zero. Without loss of generality, let  $t_{u,vw,--+}^{<k} > 0$ , so  $(uv, -) < uw- < vw+$ . We show that  $\mathbb{E}[R_{u,vw;--+}] = (1 - 1/k)^{d_{uvw} + d_{u,wv}}$ , thus showing that  $\mathbb{E}[R_{u,vw;--+}] = t_{u,vw,--+}^{<k} + t_{u,wv,--+}^{<k}$ .

Say that  $(vw, +)$  is the  $\ell^{\text{th}}$  edge to arrive. Let  $\mathcal{G}_\ell$  be the event that  $g(\ell) = 1$  and recall that  $\mathcal{E}_{NT}^{\ell-1}$  is the event that we have not yet terminated at the beginning of processing  $(vw, +)$ . Also, the underlying sketch at this time is  $\mathcal{S}_{\ell-1}$  by Lemma 10. Let  $\mathcal{F}_{--}$  be the event that  $(uv, -)$  and  $(uw, -)$  are still in  $\mathcal{S}_{\ell-1}$  conditioned on  $\mathcal{E}_{NT}^{\ell-1}$ . Since  $g$  is fully independent, we have that

$$\mathbb{P}[\mathcal{F}_{--} | \mathcal{E}_{NT}^{\ell-1}] = \mathbb{P}[(u, v, -) \in \mathcal{S}_{\ell-1}] \cdot \mathbb{P}[(u, w, -) \in \mathcal{S}_{\ell-1}] \quad (116)$$

$$= (1 - 1/k)^{d_{uvw}} \cdot (1 - 1/k)^{d_{u,wv}} \quad (117)$$

$$= (1 - 1/k)^{d_{uvw} + d_{u,wv}} \quad (118)$$

where the probabilities are due to Lemma 15.

Conditioned on  $\mathcal{F}_{--}$  and  $\mathcal{E}_{NT}^{\ell-1}$ , `query_edges` returns  $+1$  with probability  $2/|T_{\ell-1}|$  and  $\perp$  otherwise. When  $\perp$  is returned,  $R_{u,vw;--+} = 0$  by definition. Then

$$\mathbb{E}[R_{u,vw;--+} | \mathcal{F}_{--}, \mathcal{E}_{NT}^{\ell-1}, \mathcal{G}^\ell] = km \cdot \frac{2}{|\mathcal{S}_{\ell-1}|} + 0 \cdot \left(1 - \frac{2}{|\mathcal{S}_{\ell-1}|}\right) = \frac{2km}{|\mathcal{S}_{\ell-1}|} \quad (119)$$

By Lemma 14 and the random choice of  $g$ ,

$$\mathbb{P}[\mathcal{G}^\ell, \mathcal{E}_{NT}^{\ell-1}] = \mathbb{P}[\mathcal{G}^\ell] \cdot \mathbb{P}[\mathcal{E}_{NT}^{\ell-1}] = \frac{1}{k} \cdot \frac{|\mathcal{S}_{\ell-1}|}{|T_0|} = \frac{|\mathcal{S}_{\ell-1}|}{2km}. \quad (120)$$

Also note that if we do not make any queries, then  $R_{u,vw;--+} = 0$ , so  $\mathbb{E}[R_{u,vw;--+} | \overline{\mathcal{G}^\ell}] = 0$ . Using this fact along with the law of total expectation:

$$\mathbb{E}[R_{u,vw;--+} | \mathcal{F}_{--}] = \mathbb{E}[R_{u,vw;--+} | \mathcal{F}_{--}, \mathcal{E}_{NT}^{\ell-1}, \mathcal{G}^\ell] \mathbb{P}[\mathcal{E}_{NT}^{\ell-1}, \mathcal{G}^\ell | \mathcal{F}_{--}] \quad (121)$$

$$= \mathbb{E}[R_{u,vw;--+} | \mathcal{F}_{--}, \mathcal{E}_{NT}^{\ell-1}, \mathcal{G}^\ell] \mathbb{P}[\mathcal{E}_{NT}^{\ell-1}, \mathcal{G}^\ell] \quad (\text{Independent from } \mathcal{F}_{--}) \quad (122)$$

$$= \frac{2km}{|\mathcal{S}_{\ell-1}|} \cdot \frac{|\mathcal{S}_{\ell-1}|}{2km} \quad (123)$$

$$= 1. \quad (124)$$

On the other hand, conditioning on  $\overline{\mathcal{F}_{--}}$ , there are 2 possibilities: neither edge is in the sketch or one edge is in the sketch. In case 1, the query returns  $\perp$  with full probability. In case 2, the query returns  $+1$  and  $-1$  with equal probability, canceling each other out in expectation. Either way,  $\mathbb{E}[R_{u,vw;--+} | \overline{\mathcal{F}_{--}}] = 0$ .

So we conclude that

$$\mathbb{E}[R_{u,vw;--+}] = \mathbb{E}[R_{u,vw;--+} | \mathcal{F}_{--}] \mathbb{P}[\mathcal{F}_{--}] \quad (125)$$

$$= 1 \cdot (1 - 1/k) d_{uvw}^{\rightarrow} + d_{uwo}^{\rightarrow} \quad (126)$$

$$= t_{uvw,--+}^{<k} + t_{uwo,--+}^{<k}. \quad (127)$$

Therefore, no matter whether  $t_{uvw,--+}^{<k} + t_{uwo,--+}^{<k}$  is 0 or not, we have  $\mathbb{E}[R_{u,vw;--+}] = t_{uvw,--+}^{<k} + t_{uwo,--+}^{<k}$ .  $\square$

**Lemma 17.**

$$\mathbb{E}[R_{u,vw;+--}] = t_{uvw,+--}^{<k} + t_{uwo,+--}^{<k} \quad (128)$$

There is some subtlety in the subscripts on this statement but both values correspond to the triangle  $\{(uv, +), (uw, -), (vw, -)\}$  in which  $(vw, -)$  completes the triangle. Moreover, due to how these values are defined, one and only one can be non-zero but when it is, it is equal to  $(1 - 1/k) d_{uvw}^{\rightarrow} + d_{uwo}^{\rightarrow}$ . This will be helpful in the proof below.

**PROOF.** This proof is almost identical to that of Lemma 17. The main difference is that we now want the event  $\mathcal{F}_{+-}$  to be that  $(uv, +)$  and  $(uw, -)$  are still in  $\mathcal{S}_{\ell-1}$  conditioned on  $\mathcal{E}_{NT}^{\ell-1}$ . Using the

probabilities from probabilities Lemma 15, we get that

$$\mathbb{P}[\mathcal{F}_{+-} | \mathcal{E}_{NT}^{\ell-1}] = \mathbb{P}[(u, v, +) \in \mathcal{S}_{\ell-1}] \cdot \mathbb{P}[(u, w, -) \in \mathcal{S}_{\ell-1}] \quad (129)$$

$$= (1 - 1/k)^{d_{uvw}^-} \cdot (1 - 1/k)^{d_{uvw}} \quad (130)$$

$$= (1 - 1/k)^{d_{uvw}^- + d_{uvw}} \quad (131)$$

This in turn gives  $\mathbb{E}[R_{u,vw;+--}] = (1 - 1/k)^{d_{uvw}^- + d_{uvw}}$  (when it is non-zero) and thus we have  $\mathbb{E}[R_{u,vw;+--}] = t_{uvw,+--}^{<k} + t_{uvw,-+-}^{<k}$ .  $\square$

**Lemma 18.**

$$\mathbb{E}[R_{u,vw;-+-}] = t_{uvw,-+-}^{<k} + t_{uwb,+--}^{<k}. \quad (132)$$

By symmetry, this proof is identical to that of Lemma 17.

We are now able to prove that  $\mathbb{E}[R_1^{<k}] = T_1^{<k}$ .

(PROOF OF LEMMA 12). Recall that  $T_1^{<k} = T_{+--}^{<k} + T_{-+-}^{<k} + T_{--+}^{<k}$ . The goal is to show that the  $t^{<k}$  values will be counted once and only once by the algorithm. First observe that

$$\mathbb{E}[R_{--+}] = \sum_{(v < w) \in E} \sum_{u \in V} \mathbb{E}[R_{u,vw;--+}] \quad (133)$$

$$= \sum_{(v < w) \in E} \sum_{u \in V} t_{uvw,--+}^{<k} + t_{uwb,--+}^{<k} \quad (\text{Lemma 16}) \quad (134)$$

$$= \sum_{(u,v,w) \in V^3} t_{uvw,--+}^{<k} \quad (135)$$

$$= T_{--+}^{<k} \quad (136)$$

where the second-to-last line follows from the fact that for a triple  $(u, v, w) \in V^3$ , one and only one ordering may lead to a non-zero  $t_{uv,w;--+}^{<k}$  value.

We must be slightly more careful with the remaining cases. Similar to above, we can use linearity of expectation to observe the following:

$$\mathbb{E}[R_{+--}] = \sum_{(v < w) \in E} \sum_{u \in V} \mathbb{E}[R_{u,vw;+--}] = \sum_{(v < w) \in E} \sum_{u \in V} t_{uvw,+--}^{<k} + t_{uwb,+--}^{<k} \quad (\text{Lemma 17}) \quad (137)$$

$$\mathbb{E}[R_{-+-}] = \sum_{(v < w) \in E} \sum_{u \in V} \mathbb{E}[R_{u,vw;-+-}] = \sum_{(v < w) \in E} \sum_{u \in V} t_{uvw,-+-}^{<k} + t_{uwb,-+-}^{<k} \quad (\text{Lemma 18}) \quad (138)$$

We cannot ignore the ordering in each line here as we are counting slightly different triangles  $-+-$  versus  $+--$ , which depends on the edge ordering in the stream. However, by summing up the values and re-arranging, we get

$$\mathbb{E}[R_{+--}] + \mathbb{E}[R_{-+-}] = \sum_{(v < w) \in E} \sum_{u \in V} t_{uvw,+--}^{<k} + t_{uwb,+--}^{<k} + \sum_{(v < w) \in E} \sum_{u \in V} t_{uvw,-+-}^{<k} + t_{uwb,-+-}^{<k} \quad (139)$$

$$= \sum_{(u,v,w) \in V^3} t_{uv,w;+--}^{<k} + \sum_{(u,v,w) \in V^3} t_{uv,w;-+-}^{<k} \quad (140)$$

$$= T_{+--}^{<k} + T_{-+-}^{<k}. \quad (141)$$

In conclusion,  $\mathbb{E}[R_1^{<k}] = T_{+--}^{<k} + T_{-+-}^{<k} + T_{--+}^{<k} = T_1^{<k}$ .  $\square$

Next, the upper bound on the variance of  $R_1^{<k}$  is straightforward.

(PROOF OF LEMMA 13). This follows directly from  $|R_1^{<k}| \leq km$  and  $\mathbb{E}[R_1^{<k}] = T_1^{<k}$ .  $\square$

Lastly, we prove the desired performance and space bound on our median-of-means algorithm.

(PROOF OF COROLLARY 11). Recall that  $\mathbb{E}[R_1^{<k}] = T_1^{<k}$  and  $\text{Var}(R_1^{<k}) \leq (km)^2 - (T_1^{<k})^2$ .

Begin by averaging over  $N_\epsilon$  independent copies of the quantum estimator, we get a value  $\bar{X}_1$  with variance  $\text{Var}(\bar{X}_1) = \frac{\text{Var}(R_1^{<k})}{N_\epsilon} \leq \frac{(km)^2 - (T_1^{<k})^2}{N_\epsilon}$ . Using Chebyshev's inequality, we get

$$\mathbb{P}\left[\left|\bar{X}_1 - T_1^{<k}\right| \geq \epsilon T_1^{<k}\right] \leq \frac{(km)^2 - (T_1^{<k})^2}{N_\epsilon (T_1^{<k})^2} \frac{1}{\epsilon^2} \quad (142)$$

Choosing  $N_\epsilon \geq 4 \frac{(km)^2 - (T_1^{<k})^2}{(T_1^{<k})^2} \frac{1}{\epsilon^2}$  results in  $\mathbb{P}\left[\left|\bar{X}_1 - T_1^{<k}\right| \leq \epsilon T_1^{<k}\right] \geq 3/4$ .

Repeat this process  $N_\delta$  times to get estimates  $\bar{X}_{1,1}, \dots, \bar{X}_{1,N_\delta}$  and define the variable

$$\hat{X}_1 := \text{median}\left(\bar{X}_{1,1}, \dots, \bar{X}_{1,N_\delta}\right) \quad (143)$$

We are interested in understanding when  $\hat{X}_1$  is a good estimator for  $R_1^{<k}$ . Define the Bernoulli indicator variable

$$Z_j := 1 \left\{ \left| \bar{X}_{1,j} - T_1^{<k} \right| \geq \epsilon T_1^{<k} \right\} \quad (144)$$

for when estimate  $\bar{X}_{1,j}$  is bad. The median fails when over half of the estimators are bad. That is, when  $Z \geq N_\delta/2$  for  $Z := \sum_j Z_j$ . We know that  $\mathbb{E}[Z] \leq N_\delta/4$  by above. Applying Hoeffding's inequality we get

$$\mathbb{P}[Z \geq N_\delta/2] = \mathbb{P}\left[Z - \mathbb{E}[Z] \geq N_\delta/4\right] \leq \exp\left(-2N_\delta \left(\frac{1}{4}\right)^2\right) = \exp(-N_\delta/8) \quad (145)$$

Using  $N_\delta \geq 8 \ln \frac{1}{\delta}$  ensures that  $\hat{X}_1$  is good with probability  $1 - \delta$ .

In total, we need to run  $N_\epsilon \cdot N_\delta = 4 \frac{(km)^2 - (T_1^{<k})^2}{(T_1^{<k})^2} \frac{1}{\epsilon^2} \cdot 8 \ln \frac{1}{\delta} = 32 \frac{(km)^2 - (T_1^{<k})^2}{(T_1^{<k})^2} \frac{1}{\epsilon^2} \ln \frac{1}{\delta}$  iterations of the algorithm. Each iteration requires  $2 \log(n) + 2$  qubits and  $m = \mathcal{O}(\log n)$  classical bits to run. Therefore, the total space required for this overarching parallelized median-of-means algorithm is given by

$$\mathcal{O}\left(\frac{(km)^2 - (T_1^{<k})^2}{(T_1^{<k})^2} \log n \frac{1}{\epsilon^2} \log \frac{1}{\delta}\right). \quad (146)$$

$\square$